GMR
The Original

INFLUENCE OF MELATONIN AND ITS AGONIST ON HISTOPATHOLOGICAL CHANGES OF THYROID, SPLEEN AND ADRENAL GLANDS IN FUNCTIONAL AND STRUCTURAL PINEALECTOMIZED RATS

Hero Khalid Mustafa

Basic Science. Anatomy and Pathology Department, College of Medicine, Hawler Medical University, Iraq
Corresponding Author E-mail: hero.khalid@hmu.edu.krd

ABSTRACT
The pineal gland, through its secretion of melatonin, plays a central role in regulating circadian rhythms, oxidative balance, and immune-endocrine homeostasis. Disruption of pineal activity by continuous light exposure or surgical pinealectomy has been shown to induce oxidative stress, tissue degeneration, and immune dysregulation in peripheral organs. The present study investigated the histopathological and immunohistochemical changes in the thyroid gland, adrenal glands, and spleen of adult male albino rats following pinealectomy and continuous light exposure, and further evaluated the protective effects of melatonin and its receptor agonist, ramelteon. Seventy five rats were divided into control, pinealectomy, continuous light, melatonin-treated, and ramelteon-treated groups and maintained under standard laboratory conditions for a 10-week experimental period. Histological examination revealed that both continuous light and pinealectomy induced profound architectural alterations, including follicular disorganization and colloid depletion in the thyroid, cortical vacuolation and chromaffin cell damage in the adrenal glands, and necrosis, congestion, and hemorrhage in the spleen. These changes were accompanied by marked increases in CD163-positive macrophage expression, indicating enhanced inflammatory and immune responses. Treatment with melatonin partially preserved tissue integrity by maintaining follicular and cortical structures and reducing immune cell infiltration. Notably, ramelteon demonstrated comparable, and in some cases stronger, protective effects, restoring near-normal histological features in adrenal and splenic tissues and suppressing CD163 immunoreactivity to lower levels. Together, these findings highlight the essential role of pineal-derived melatonin in maintaining circadian rhythm–dependent endocrine and immune functions. Moreover, they emphasize the therapeutic potential of melatonin receptor agonists such as ramelteon as clinical alternatives in conditions associated with circadian disruption, oxidative injury, and immune imbalance.
KEYWORDS: Pineal gland; melatonin; ramelteon; pinealectomy; continuous light exposure.

INTRODUCTION

The pineal gland, a small neuroendocrine organ located near the brain's center, plays a pivotal role in regulating circadian rhythms through its secretion of melatonin, a hormone synchronized with the light-dark cycle [1], Melatonin (N-acetyl-5-methoxytryptamine), derived from tryptophan, exhibits peak secretion during the night and declines under light exposure, thereby acting as a major chronobiotic that stabilizes the body's internal clock [2]. Its synthesis is regulated by adrenergic receptors and cyclic AMP signaling, which activates aralkylamine N-acetyltransferase, the rate-limiting enzyme in melatonin production [3]. Beyond its chronobiological role, melatonin exerts extensive antioxidant and anti-inflammatory actions. It directly neutralizes reactive oxygen and nitrogen species while simultaneously upregulating enzymatic antioxidants such as superoxide dismutase (SOD), glutathione peroxidase (GPx), and catalase [4]. At the molecular level, melatonin suppresses the nuclear factor-kappa B (NF-κB) pathway, resulting in reduced expression of pro-inflammatory mediators like tumor necrosis factor-alpha (TNF-α) and interleukin-1β (IL-1β), thereby limiting inflammation-induced tissue damage [5]. Moreover, circadian control of mitochondrial metabolic and antioxidant enzymes has been demonstrated, highlighting the importance of melatonin in maintaining redox balance [6]. Disruption of this balance, as occurs with pinealectomy (PX), leads to oxidative stress, impaired antioxidant defenses, and activation of pro-oxidative pathways, contributing to tissue injury and accelerated aging [7]. Experimental PX models have revealed profound structural and functional changes in multiple organs, including the liver, kidneys, brain, adrenal glands, thyroid, and spleen [8]. The adrenal glands, which regulate stress responses through cortisol secretion, are particularly influenced by pineal-adrenal crosstalk, with pineal dysfunction leading to altered adrenal cortex activity, oxidative imbalance, and histopathological alterations [9]. Similarly, the thyroid gland demonstrates sensitivity to oxidative stress and inflammation; melatonin has been shown to protect thyroid follicular architecture, reduce apoptosis, and modulate lipid peroxidation through receptor-mediated mechanisms [10]. The spleen, a central immune organ, also reflects melatonin's immunomodulatory properties. PX-induced architectural disorganization and increased apoptosis in the spleen can be mitigated by melatonin supplementation, which preserves white pulp integrity and reduces macrophage activation [11]. Given these observations, melatonin deficiency due to pinealectomy serves

as a valuable model to study the systemic consequences of circadian disruption. The use of melatonin and its synthetic agonist, ramelteon, offers promising therapeutic avenues for protecting peripheral organs against oxidative and inflammatory injury triggered by pineal dysfunction. Therefore, the present study investigates the histopathological effects of melatonin and ramelteon on the thyroid, adrenal glands, and spleen of pinealectomized rats, aiming to elucidate the protective roles of chronobiotic agents in maintaining organ integrity under conditions of circadian rhythm disruption.

MATERIALS AND METHODS

Animals and housing

Adult male albino rats (*Rattus norvegicus*), weighing between 150–250 g, were used in this study. Animals were housed in plastic cages under standard laboratory conditions in the Animal House of the Department of Biology, College of Science, Salahaddin University-Erbil. Rats were maintained on a standard diet containing wheat (66.6%), soya (25.6%), corn oil (4.4%), limestone (1.5%), salt (0.63%), methionine (0.158%), lysine (0.24%), choline chloride (0.062%), multivitamins (0.5%), and trace elements (0.05%) (Mahmood et al., 2025), with tap water provided *ad libitum*. Environmental conditions were controlled at 22 ± 4 °C with a 12/12 h light/dark cycle. The Animal Research Ethic Committee (AREC) confirmed that the current study belonged to the College of Science, Salahaddin University-Erbil, Erbil, Iraq (Reference number 45177 and Date of Issue: April 30, 2025).

Body weight

Body weights were recorded biweekly using an electronic balance. Weight gain was calculated as the ratio of weekly weight increase to initial body weight.

Preparation of melatonin dose

Melatonin was obtained from Solarbio Life Science Company (China). For the continuous light model, 0.1 g of pure melatonin was suspended in 1% normal saline, shaken thoroughly, and administered daily by gavage. For the pinealectomy model, melatonin was dissolved in 1% ethanol and diluted with tap water to a final concentration of 100 ml, which was provided as drinking water.

Preparation of ramelteon dose

Ramelteon was purchased from Ramelda-ABDI IBRAHIM (Maslak, Istanbul). For the continuous light model, tablets containing 8 mg ramelteon were suspended in 1% normal saline, shaken, and administered daily by gavage. For the pinealectomy model, tablets were dissolved in 1% ethanol and diluted with tap water to a final concentration of 100 ml, which was used as drinking water.

Experimental design

The experimental design consisted of two models conducted over a 10-week treatment period. In Experiment I (Continuous Light Exposure Model), 35 rats were divided into four groups: the control group (n=8) was maintained under a 12/12 h light–dark cycle with standard diet and water; the continuous light group (n=8) was exposed to LED light continuously (24 h/day, >600 lux) with standard diet and water; the continuous light + melatonin group (n=9) was exposed to continuous LED light and administered melatonin (10 mg/kg body weight, gavage) daily between 09:00–11:00 AM; and the continuous light + ramelteon group (n=10) was exposed to continuous LED light and administered ramelteon (10 mg/kg body weight, gavage) daily between 09:00–11:00 AM. In Experiment II (Pinealectomy Model), 40 rats were divided into five groups: the control group (n=7) was kept under a 12/12 h light–dark cycle with standard diet and tap water containing 1% ethanol; the pinealectomy group (n=8) underwent surgical removal of the pineal gland and received standard diet with tap water (1% ethanol); the pinealectomy + melatonin group (n=7) underwent pinealectomy and received melatonin (10 mg/kg body weight, dissolved in 0.1% ethanol and diluted in 100 ml tap water) with standard diet; the pinealectomy + ramelteon group (n=9) underwent pinealectomy and received ramelteon (10 mg/kg body weight, dissolved in 0.1% ethanol and diluted in 100 ml tap water) with standard diet; and the pinealectomy + continuous light group (n=9) underwent pinealectomy and was exposed to continuous LED light (24 h/day, >600 lux) with standard diet and tap water (1% ethanol).

Pinealectomy procedure

Pinealectomy was performed following the technique of Hoffman and Reiter (1965). Rats were anesthetized intraperitoneally with a ketamine (90 mg/kg) and xylazine (10 mg/kg) mixture. A partial square craniotomy was drilled, and the bone flap was folded anteriorly. The pineal gland was excised after incision of the superior sagittal sinus using fine-tipped forceps. The bone flap was replaced, the scalp was closed with surgical staples, and the wound was treated with procaine penicillin powder. Post-surgery, rats received tetracycline antibiotics in drinking water for one week during recovery.

Dissection and organ collection

The rats were dissected, and the thyroid ,spleen and adrenal glands were excised. Organs were weighed using a precision electronic balance (BL-220H, Shimadzu, Japan) and fixed in 10% formal saline.

Histological procedure
Thyroid ,spleen and adrenal tissues were fixed in 10% formalin, dehydrated through graded ethanol (50%, 70%, 95%, 100%), cleared in xylene, and embedded in paraffin wax. Tissue sections (4 µm) were prepared using a rotary microtome (Bright, MIC) and stained with hematoxylin and eosin (H&E). Slides were examined and photographed under a light microscope at 40×–2000× magnification with a built-in 3 MP USB camera.

Immunohistochemistry
Immunohistochemical analysis was performed to detect CD163-positive macrophages in thyroid spleen and adrenal tissues following the method of Matsuyama et al. (2018) with modifications. Sections (4 µm) were mounted on poly-L-lysine-coated slides and incubated overnight at 37 °C. After deparaffinization, rehydration, and phosphate-buffered saline (PBS) rinses, antigen retrieval was achieved in 0.01 M citrate buffer (pH 6.0) by microwave heating for 15 min. Endogenous peroxidase activity was blocked with 3% hydrogen peroxide, followed by blocking with 5% skimmed milk. Sections were incubated with mouse monoclonal anti-CD163 antibody (ED2 clone, 1:300, AbD Serotec, Oxford, UK) for 1 h at room temperature, then with horseradish peroxidase-conjugated secondary antibody (Histofine Simple Stain MAX-PO®, Nichirei Biosciences Inc., Tokyo, Japan) for 30 min. Visualization was achieved with 3,3′-diaminobenzidine (DAB) substrate (Vector Laboratories, Burlingame, CA, USA). Slides were counterstained with Mayer's hematoxylin, dehydrated, cleared in xylene, and mounted in DPX. Negative controls were prepared by substituting the primary antibody with non-immune mouse serum.

RESULTS
Effect of melatonin on thyroid gland texture of rats exposed to continuous light
In the control rats, histological sections of the thyroid gland showed normal follicular architecture, with follicles of variable sizes (black arrows), each lined by a single layer of cuboidal follicular cells (blue arrows) containing acidophilic colloid (red arrows). The follicles were surrounded by interfollicular connective tissue with distinct blood vessels (green arrows), confirming preserved glandular structure (Figure 1A–B). In contrast, rats exposed to continuous light exhibited microfollicular follicles with markedly reduced colloid content (black arrows) and cellular ingrowth projecting into the follicular lumen (blue arrows). The epithelial lining transformed into multiple layers of tall columnar cells with dark nuclei (red arrows), and interfollicular regions displayed congested blood vessels (green arrows) together with vacuolated colloid (Figure 1C–D).

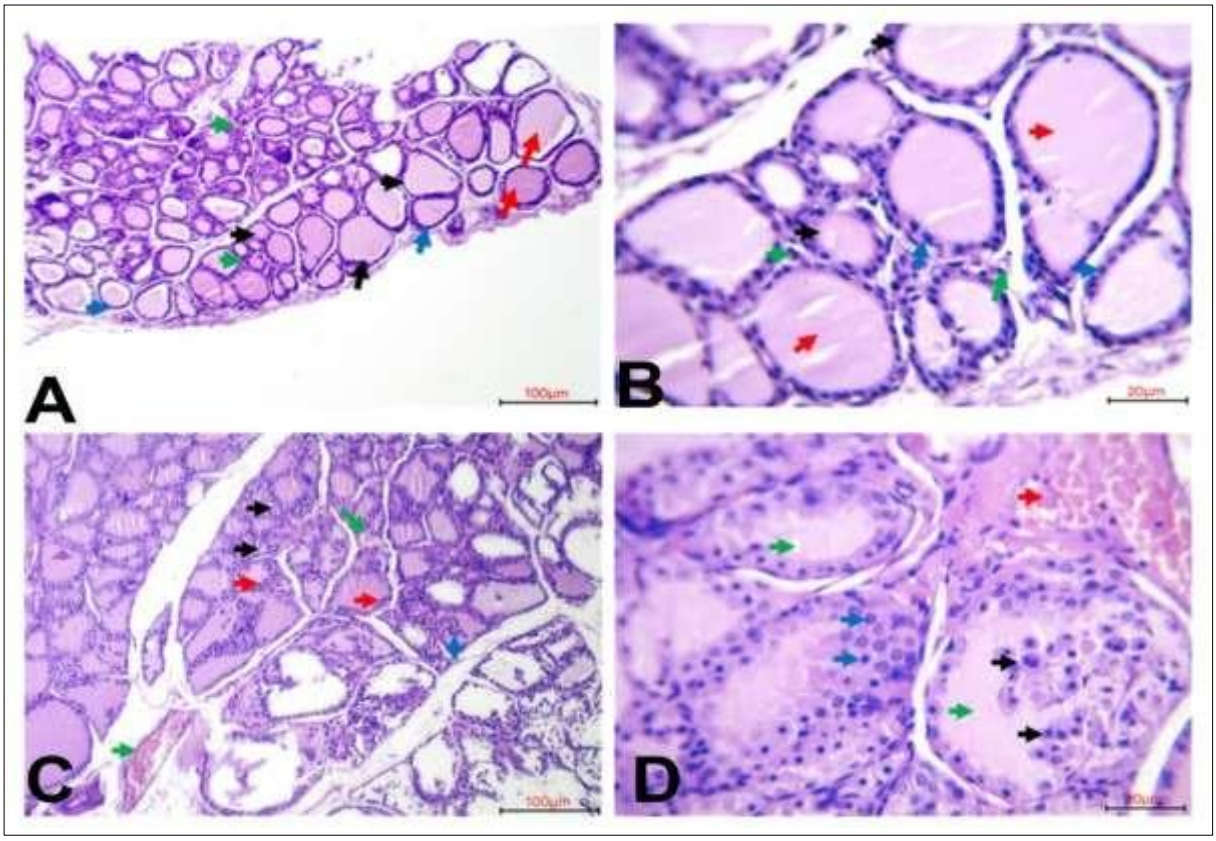

Figure 1. Histological sections of the thyroid gland in control and continuous light–exposed rats. (A–B) Sections from control rats showing normal variable follicle size (black arrows), lined by a single layer of cuboidal follicular cells (blue arrows) containing acidophilic colloid (red arrows). The follicles were surrounded by interfollicular tissue with blood vessels (green arrows).(H&E,100µm). (C) Section from rats exposed to continuous light showing microfollicular follicles with reduced colloid content (black arrows) and cellular

ingrowth projecting into the lumen (blue arrows). Follicles were lined by multiple layers of tall columnar cells with dark nuclei (red arrows) and congested blood vessels between follicles (green arrows). (H&E, 100 µm).
(D) Section from rats exposed to continuous light showing follicular lumen with cell ingrowth (black arrows), multiple layers of tall columnar cells with dark nuclei (blue arrows), congested blood vessels (red arrows), and vacuolated acidophilic colloid. (H&E, 20 µm).

In rats treated with melatonin after exposure to continuous light, the thyroid gland largely preserved its normal histological features. Most follicles were lined by a single layer of cuboidal follicular cells (black arrows), although some showed multilayered epithelial lining (blue arrows) or were lined by flattened cells (red arrow). Dilated and congested blood vessels were also visible in the interfollicular areas (green arrows), reflecting partial vascular alterations (Figure 2A). In other sections, melatonin treatment maintained follicular organization close to normal, with follicles of variable sizes lined by a cuboidal epithelium (black arrows) and colloid content appearing intact (Figure 2B).

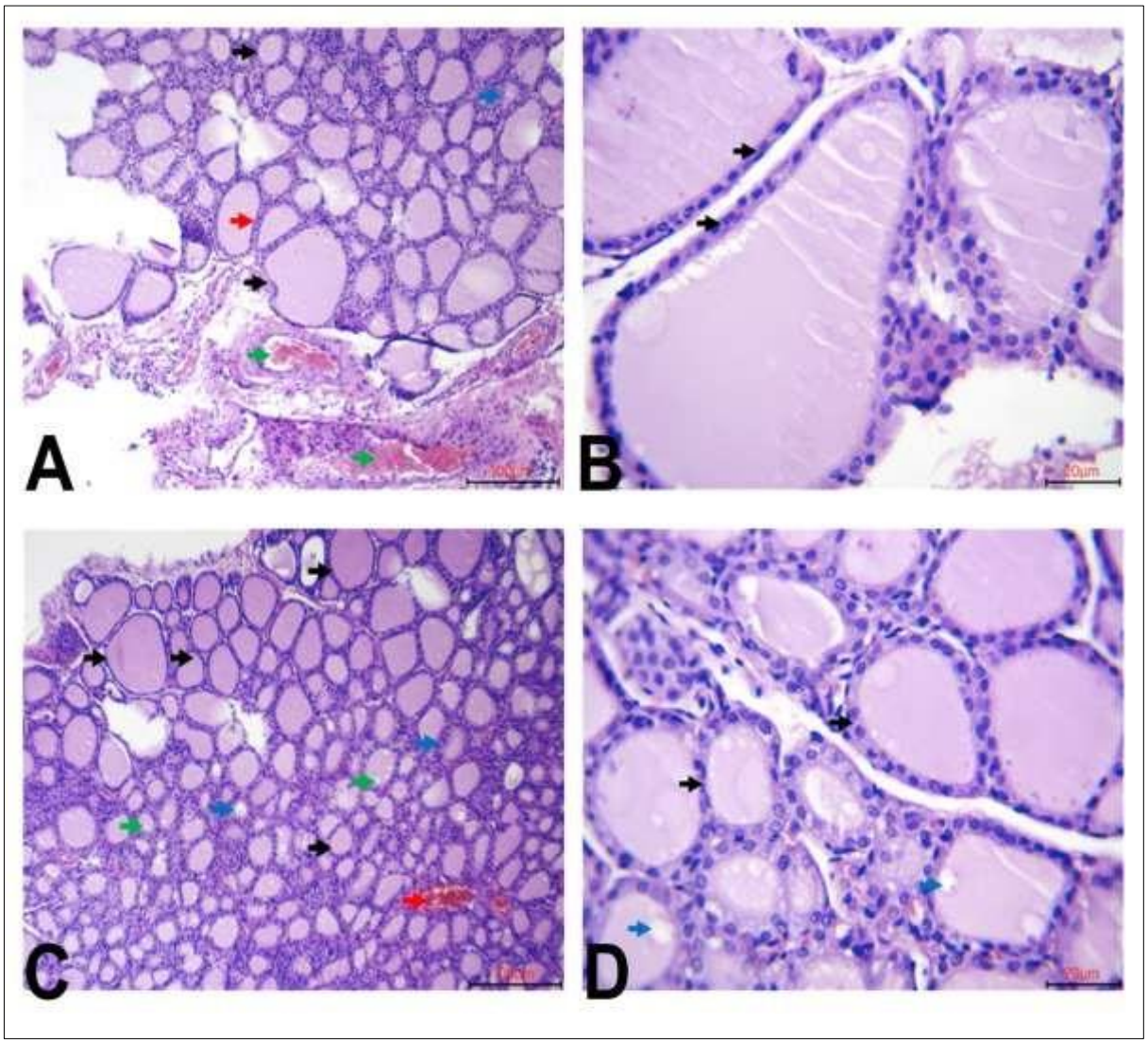

Figure 2. Histological sections of the thyroid gland in rats exposed to continuous light and treated with melatonin or ramelteon.(A) Section from rats treated with melatonin (10 mg/kg) showing thyroid follicles, most lined by a single layer of cuboidal cells (black arrows), while some exhibit several cellular layers (blue arrows) or are lined by flat cells (red arrow). Dilated congested blood vessels are also visible (green arrow). (H&E, 100 µm).
(B) Section from melatonin-treated rats showing normal thyroid follicles lined by a single layer of cuboidal cells (black arrows). (H&E,20µm). (C) Section from ramelteon-treated rats showing thyroid follicles of variable sizes, lined by a single layer of cuboidal cells (black arrows). Some follicles exhibit multilayered cellular lining (blue arrows), with congested blood vessels between follicles (red arrow) and few vacuolated colloids (green arrows). (H&E, 100 µm).
(D) Section from ramelteon-treated rats showing variable-sized follicles, all lined by a single layer of cuboidal cells (black arrows), with minimal colloid vacuolation (blue arrows). (H&E, 20 µm).

Effect of melatonin on adrenal gland texture of rats exposed to continuous light

In the control rats, histological sections of the adrenal gland revealed normal architecture, including the capsule of dense irregular connective tissue containing smooth muscle (black arrow), a well-organized zona glomerulosa (blue arrow), zona fasciculata (red arrows), zona reticularis (green arrow), and normal chromaffin cells with intact nuclei and cytoplasm (yellow arrow), confirming preserved cortical and medullary structures (Figure 3A). In contrast, rats exposed to continuous light exhibited distinct pathological alterations. Sections showed cortical hyperplasia (blue arrow), vacuolation of cells within the zona glomerulosa and zona fasciculata (black arrows), disorganization of the normal radial arrangement, and cells undergoing karyolysis (red arrows). Additionally, chromaffin cells in the adrenal medulla appeared vacuolated, reflecting structural and functional stress (green arrows) (Figure 3B). More severe changes were evident in other sections of continuous light–exposed rats, where the zona fasciculata displayed extensive vacuolation (black arrows), disrupted radial cellular arrangement, and widespread nuclear degeneration with karyolysis (blue arrows). Chromaffin cells showed prominent vacuolation and pyknosis, indicating advanced degenerative changes (green arrows) (Figure 3C).

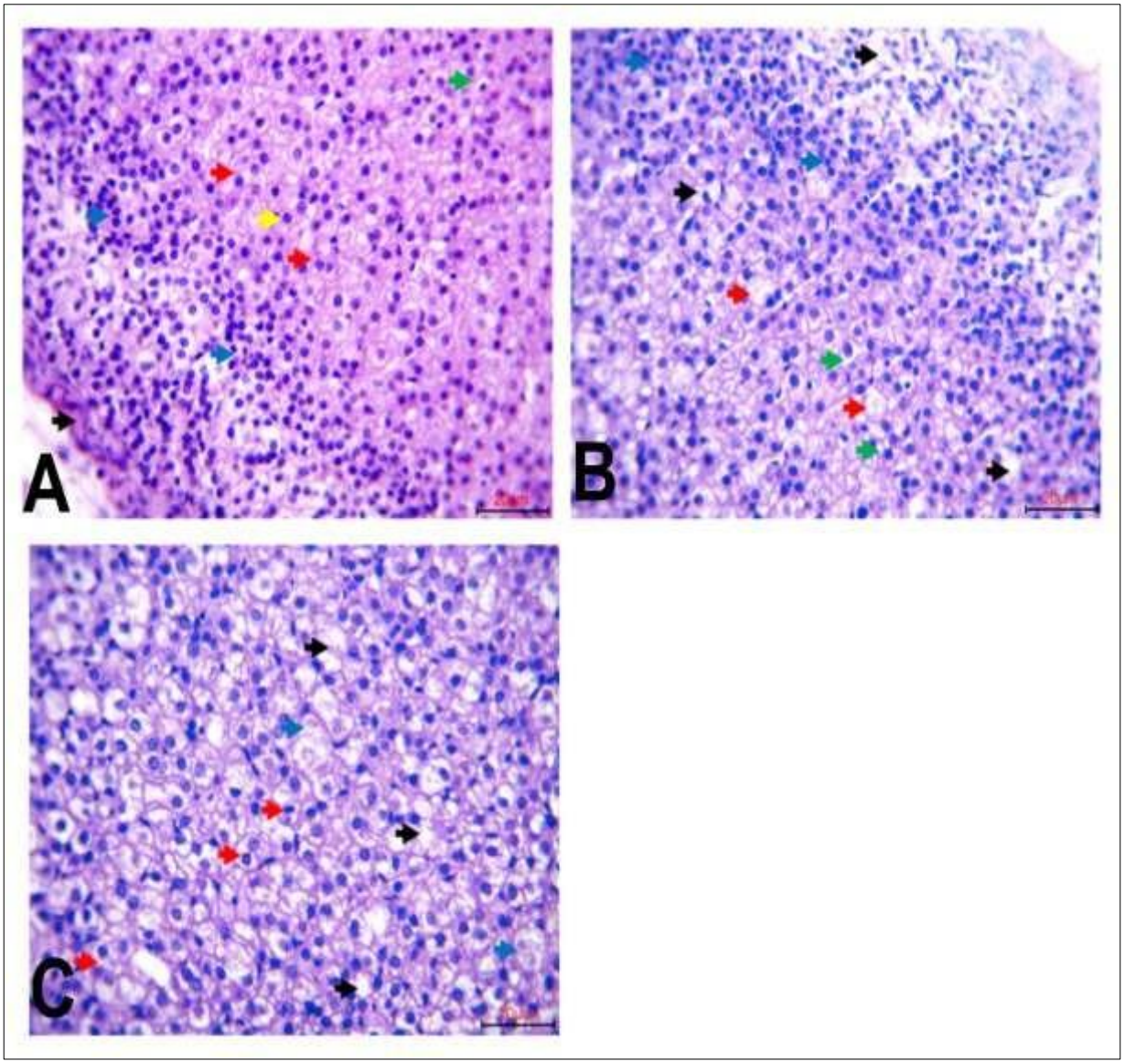

Figure 3. Histological sections of the adrenal gland in control and continuous light–exposed rats. (A) Section from control rats showing normal adrenal architecture, including the capsule of dense irregular connective tissue containing smooth muscle (black arrow), zona glomerulosa (blue arrow), zona fasciculata (red arrows), zona reticularis (green arrow), and normal chromaffin cells (yellow arrow). (H&E, 20 µm).
(B) Section from rats exposed to continuous light showing hyperplasia (blue arrow), vacuolation of the zona glomerulosa and zona fasciculata (black arrows), disrupted radial arrangement, and cells with karyolysis (red arrows). Vacuolated chromaffin cells are also evident (green arrows). (H&E, 20 µm).
(C) Section from rats exposed to continuous light showing severe vacuolation of the zona fasciculata (black arrows), disrupted radial arrangement, and cells with karyolysis (blue arrows). Chromaffin cells display vacuolation and pyknosis (green arrows). (H&E, 20 µm).

In rats exposed to continuous light but treated with melatonin, adrenal cortical structures showed marked hyperplasia within the zona granulosa and zona fasciculata (blue arrows). Some chromaffin cells retained normal cytoplasm and nuclei (black arrow), whereas others displayed cytoplasmic vacuolation (red arrows), indicating partial but not complete protection (Figure 4A). In other sections, melatonin treatment preserved the cortical zones, with well-defined zona granulosa and zona fasciculata (black arrows), thickened connective tissue capsules (blue arrow), chromaffin cells exhibiting normal cytoplasm and nuclei (red arrow), and the presence of normal lipid droplets (green arrows), though mild cytoplasmic vacuolation persisted (yellow arrows) (Figure 4B). Rats treated with ramelteon demonstrated stronger preservation of adrenal gland histology. Sections showed normal architecture with the capsule of dense connective tissue containing smooth muscle (black arrow), intact zona glomerulosa (blue arrow), zona fasciculata (red arrow), and chromaffin cells that appeared normal, with a regular distribution of lipid droplets (yellow arrows) (Figure 4C). In additional sections, ramelteon-treated rats maintained nearly normal adrenal cortical organization, including the capsule of dense irregular connective tissue with smooth muscle (black arrow), and well-preserved zona glomerulosa (blue arrow), zona fasciculata (red arrow), and chromaffin cells (green arrow) (Figure 4D).

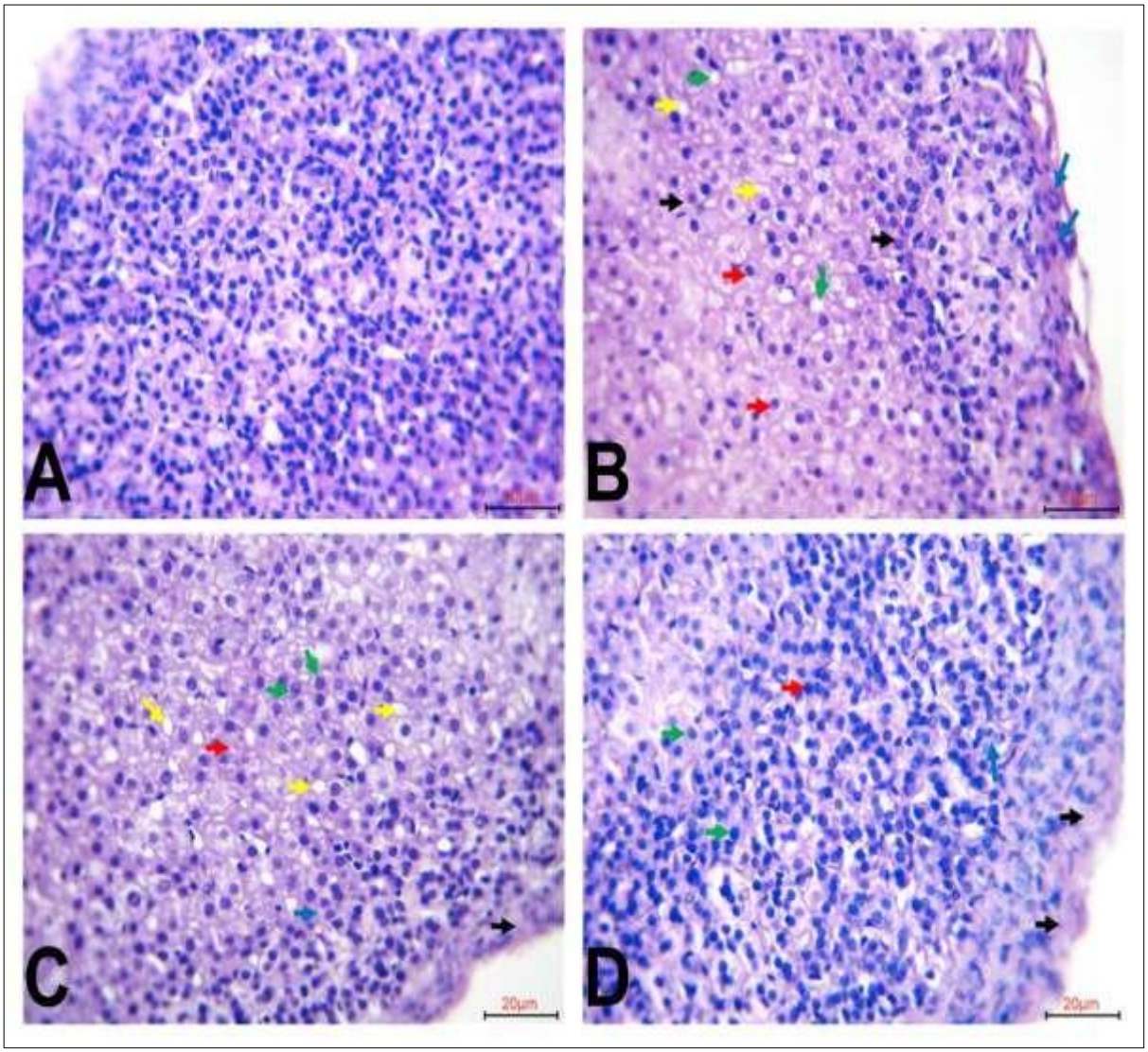

Figure 4. Histological sections of the adrenal gland in rats exposed to continuous light and treated with melatonin or ramelteon.(A) Section from melatonin-treated rats (10 mg/kg) showing severe hyperplasia in adrenal cortical structures, including the zona granulosa and zona fasciculata (blue arrows). Some chromaffin cells exhibit normal cytoplasm and nuclei (black arrow), while others show cytoplasmic vacuolation (red arrows). (H&E, 20 μm). (B) Section from melatonin-treated rats showing preserved adrenal cortical architecture with zona granulosa and zona fasciculata (black arrows), thickening of connective tissue capsules (blue arrow), chromaffin cells with normal cytoplasm and nuclei (red arrow), normal lipid droplets (green arrows), and cytoplasmic vacuolation in some chromaffin cells (yellow arrows). (H&E, 20 μm). (C) Section from ramelteon-treated rats (10 mg/kg) showing normal adrenal architecture. The capsule of dense irregular connective tissue contained smooth muscle (black arrow). The zona glomerulosa (blue arrow), zona fasciculata (red arrow), and chromaffin cells (green arrow) appeared normal, with a regular distribution of lipid droplets (yellow arrows). (H&E, 20 μm). (D) Section from

ramelteon-treated rats showing normal adrenal architecture, including capsule of dense irregular connective tissue with smooth muscle (black arrow), zona glomerulosa (blue arrow), zona fasciculata (red arrow), and normal chromaffin cells (green arrow). (H&E, 20 µm).

Effect of continuous light on spleen texture

In the control rats, histological sections of the spleen showed normal splenic organization with distinct red pulp (black arrows), white pulp or splenic nodules (blue arrows), a well-defined central artery (red arrow), and clearly visible germinal centers (green arrows), confirming intact splenic architecture (Figure 5A–B). By contrast, rats exposed to continuous light displayed notable vascular and architectural disruptions. Sections revealed a thick-walled central arteriole with a narrowed lumen and mild vacuolar degeneration within the vessel wall (black arrows). In addition, dilatation of the sinusoids was observed within the red pulp (blue arrows), indicating early degenerative and circulatory changes (Figure 5C). In other sections, continuous light exposure further caused thickened central arterioles (black arrows) accompanied by mild vacuolar degeneration in the arteriole walls (blue arrows), reflecting compromised vascular integrity (Figure 5D).

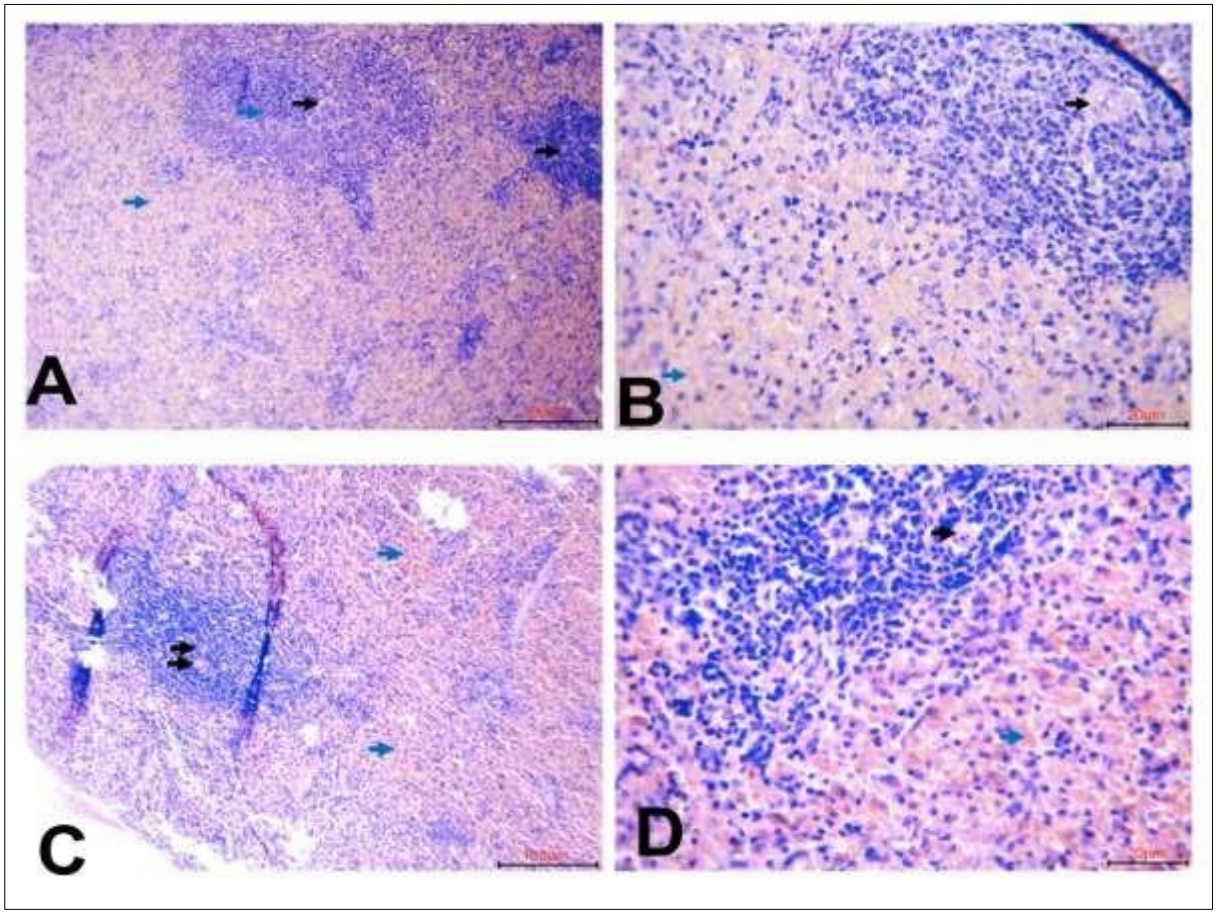

Figure 5. Histological sections of the spleen in control and continuous light–exposed rats. (A–B) Sections from control rats showing normal splenic architecture with distinct red pulp (black arrow), white pulp or splenic nodule (blue arrow), central artery (red arrow), and germinal center (green arrow). (H&E, 100 µm and 20 µm).
(C) Section from rats exposed to continuous light showing a thick-walled and narrow-lumened central arteriole with mild vacuolar degeneration in the vessel wall (black arrows), along with dilatation of the sinusoids within the red pulp (blue arrows). (H&E, 100 µm). (D) Section from rats exposed to continuous light showing thickened central arterioles (black arrows) with mild vacuolar degeneration in the arteriole (blue arrows). (H&E, 20 µm).

In rats treated with melatonin following continuous light exposure, the spleen displayed preserved structural features. Sections showed normal central arterioles (black arrows), distinct germinal centers (blue arrow), and well-maintained sinusoids within the red pulp (blue arrows), suggesting protective effects of melatonin on splenic microarchitecture (Figure 6A). In other sections, melatonin treatment maintained central arterioles (black arrows) with intact red pulp sinusoids (blue arrows), supporting vascular and tissue preservation despite light-induced stress (Figure 6B). Rats treated with ramelteon exhibited comparable, and in some cases stronger, protective outcomes. Sections revealed normal central arterioles (black arrows) and intact red pulp sinusoids (blue arrows), maintaining near-normal splenic organization (Figure 6C). Further sections confirmed this preservation, as ramelteon maintained well-structured central arterioles (black arrows) together with red pulp sinusoids (blue arrows), reflecting effective protection against vascular and parenchymal injury (Figure 6D).

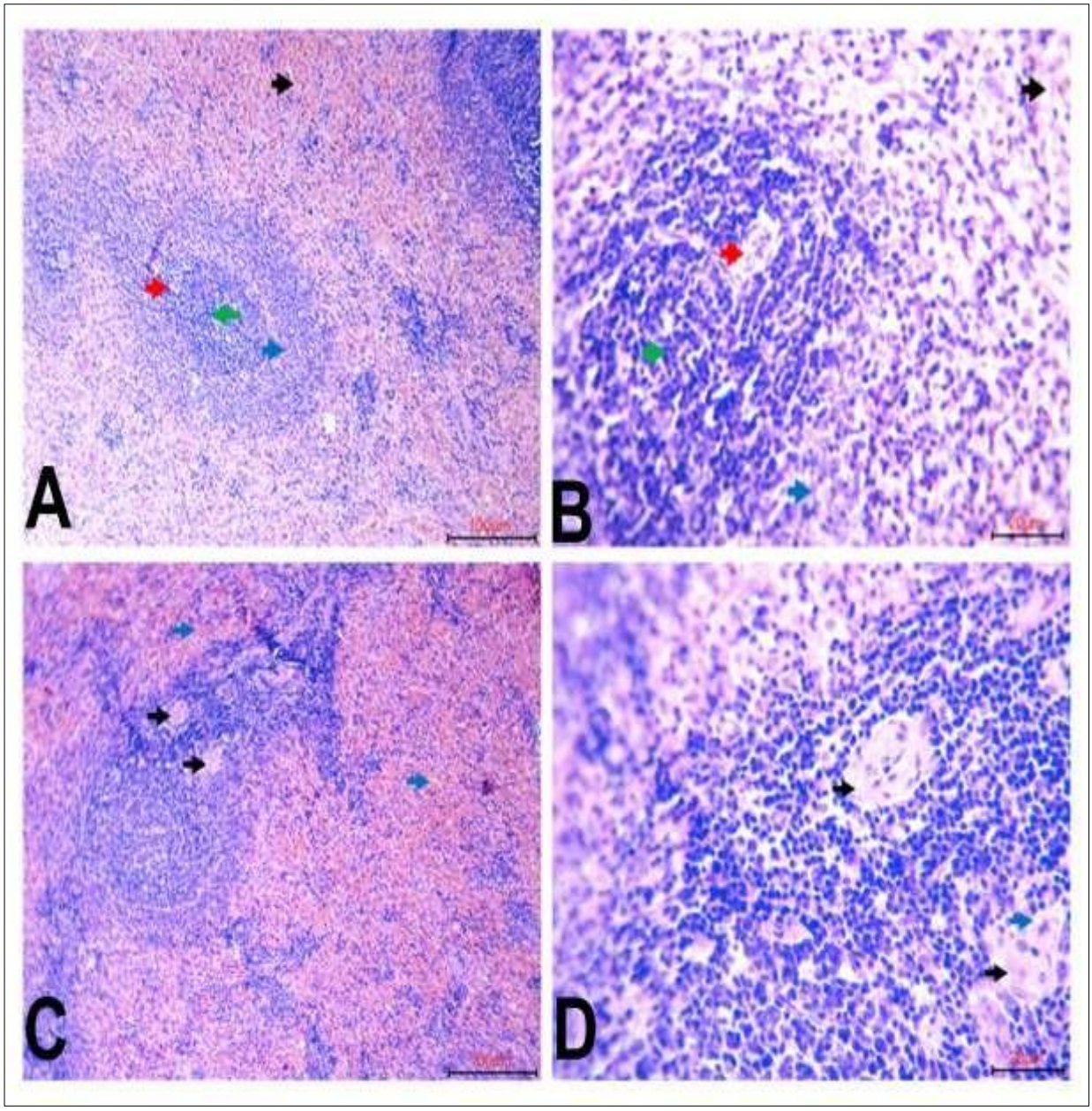

Figure 6. Histological sections of the spleen in rats exposed to continuous light and treated with melatonin or ramelteon**.** (A) Section from melatonin-treated rats (10 mg/kg) showing a normal central arteriole (black arrow), germinal center (blue arrow), and normal sinusoids within the red pulp (blue arrows). (H&E, 100 µm). (B) Section from melatonin-treated rats showing normal central arterioles (black arrows) and well-preserved sinusoids within the red pulp (blue arrows). (H&E, 20 µm). (C) Section from ramelteon-treated rats (10 mg/kg) showing normal central arterioles (black arrows) and intact sinusoids within the red pulp (blue arrows). (H&E, 100 µm). (D) Section from ramelteon-treated rats showing normal central arterioles (black arrows) and preserved red pulp sinusoids (blue arrows). (H&E, 20 µm).

The CD163 immunoreactivity in the thyroid gland under continuous light and treatment

In the control rats, thyroid sections showed negative CD163 expression, with no brown immunostaining detected in the follicular tissue, confirming the absence of macrophage infiltration (Figure 7A). In contrast, rats exposed to continuous light demonstrated moderate CD163 positivity, visible as brown-stained infiltrating macrophages around the thyroid follicles (black arrows), indicating inflammatory activation (Figure 7B). Melatonin treatment reduced this inflammatory response, with thyroid sections showing weak CD163 positivity, where only a few infiltrating macrophages stained brown (black arrows) (Figure 7C). Rats treated with ramelteon exhibited even lower immunoreactivity, with very weak CD163 expression detected in occasional macrophages, reflecting stronger suppression of immune activation (Figure 7D).

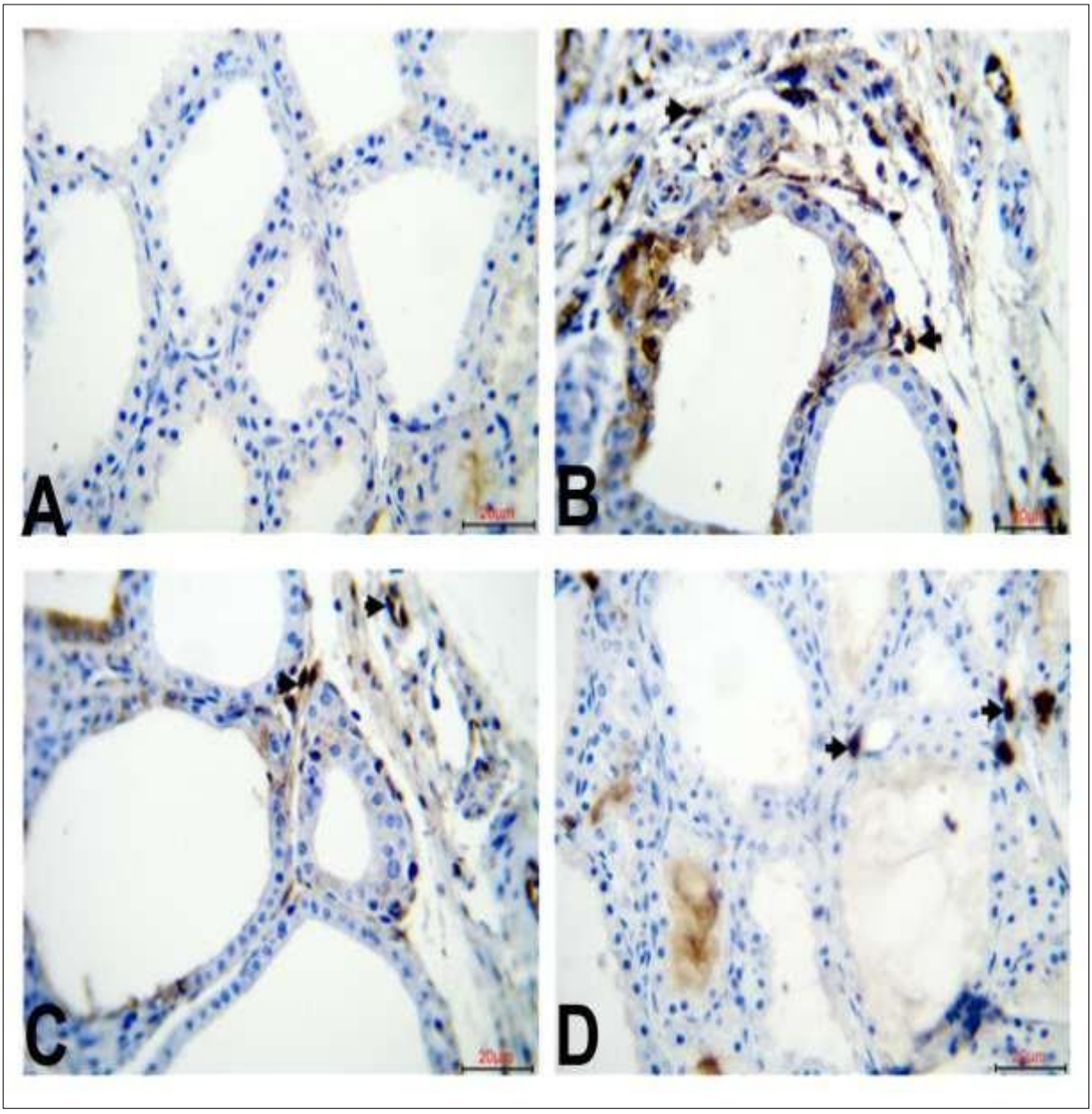

Figure 7. Immunohistochemical staining for CD163 in thyroid glands of control and experimental rats**.** (A) Control rats showing negative expression (–) of CD163 in thyroid tissue. (IHC, 20 µm). (B) Rats exposed to continuous light showing moderate positive immunoreactivity (++) of CD163, visible as brown staining in infiltrating macrophages (black arrows). (IHC, 20 µm). (C) Rats exposed to continuous light and treated with melatonin (10 mg/kg) showing weak positive immunoreactivity (+) of CD163 in infiltrating macrophages (black arrows). (IHC, 20 µm).
(D) Rats exposed to continuous light and treated with ramelteon (10 mg/kg) showing very weak immunoreactivity (±) of CD163 in infiltrating macrophages (black arrows). (IHC, 20 µm).

The CD163 immunoreactivity in the adrenal gland under continuous light and treatment

In the control rats, adrenal gland tissue showed negative CD163 expression, with no brown immunostaining detected, indicating the absence of macrophage activation (Figure 8A). In contrast, rats exposed to continuous light exhibited low positive immunoreactivity, demonstrated by brown-stained infiltrating macrophages (black arrows) within the adrenal tissue, reflecting the onset of inflammatory responses (Figure 8B). Treatment with melatonin reversed this change, as adrenal sections showed negative CD163 expression, suggesting suppression of macrophage activity and restoration of near-normal tissue conditions (Figure 8C). Similarly, rats treated with ramelteon also exhibited negative CD163 expression, with no observable immunostaining, indicating strong protection against light-induced immune activation (Figure 8D).

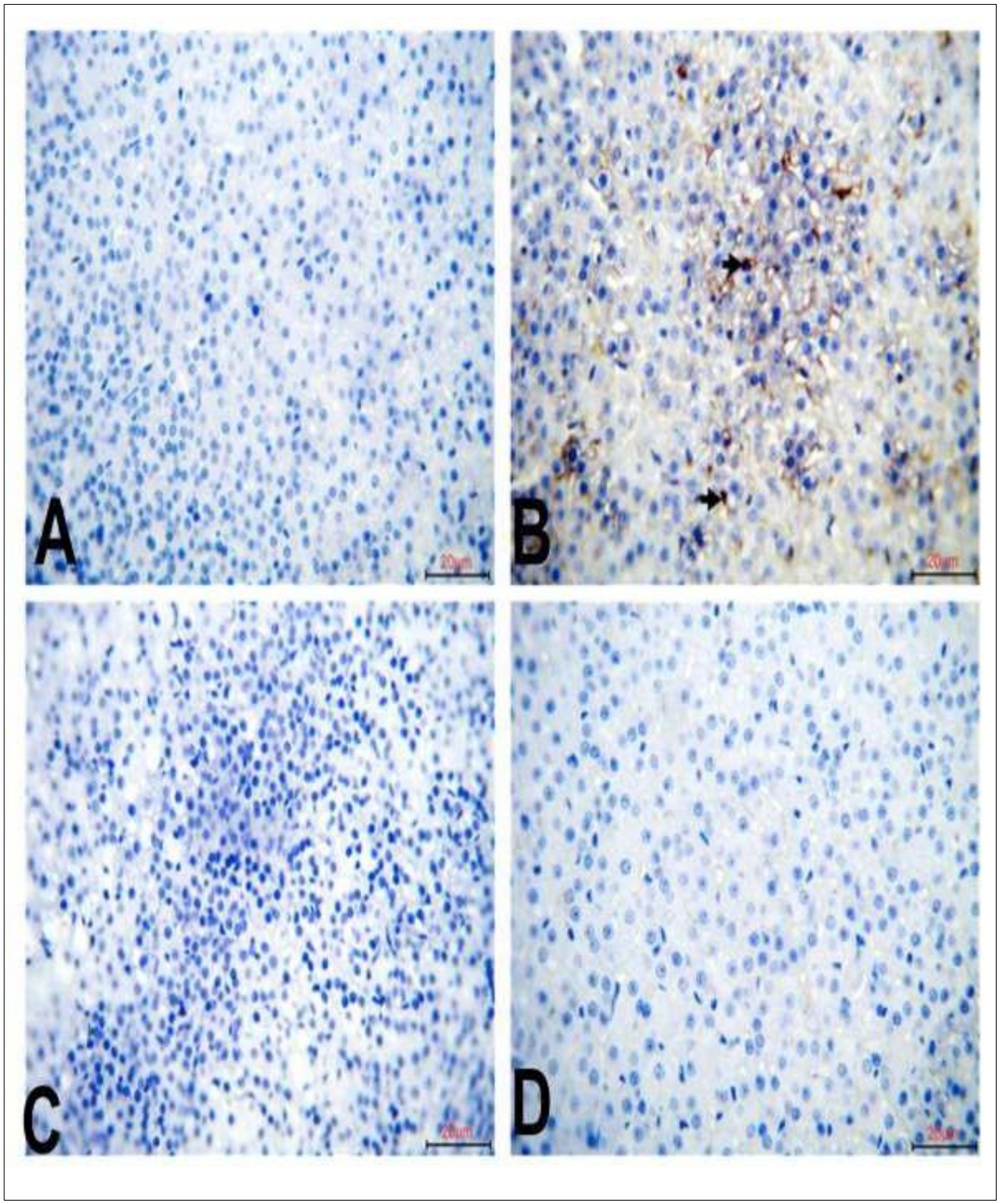

Figure 8. Immunohistochemical staining for CD163 in adrenal glands of control and experimental rats. (A) Control rats showing negative expression (–) of CD163 in adrenal gland tissue. (IHC, 20 µm). (B) Rats exposed to continuous light showing low positive immunoreactivity (+) of CD163, observed as brown staining in infiltrating macrophages (black arrows). (IHC, 20 µm). (C) Rats exposed to continuous light and treated with melatonin (10 mg/kg) showing negative expression (–) of CD163 in adrenal gland tissue. (IHC, 20 µm). (D) Rats exposed to continuous light and treated with ramelteon (10 mg/kg) showing negative expression (–) of CD163 in adrenal gland tissue. (IHC, 20 µm).

The CD163 immunoreactivity in the spleen under continuous light and treatment

In the control rats, spleen sections showed very high CD163 immunoreactivity (++++), evident as brown staining of a normal subset of resident splenic macrophages within the red pulp (black arrows), reflecting baseline immune activity (Figure 9A). Continuous light exposure markedly increased this expression, with very high CD163 positivity (++++), localized in splenic macrophages of the red pulp, showing more intense staining compared with the control group (Figure 9B). Following melatonin treatment, CD163 expression remained very high (++++), but the intensity was reduced compared with the untreated continuous light group, indicating partial suppression of macrophage activation (black arrows) (Figure 9C). Ramelteon treatment also maintained very high

immunoreactivity (++++), but expression was significantly reduced compared with continuous light exposure alone, showing stronger modulation of macrophage activity (Figure 9D; Table 1, 2).

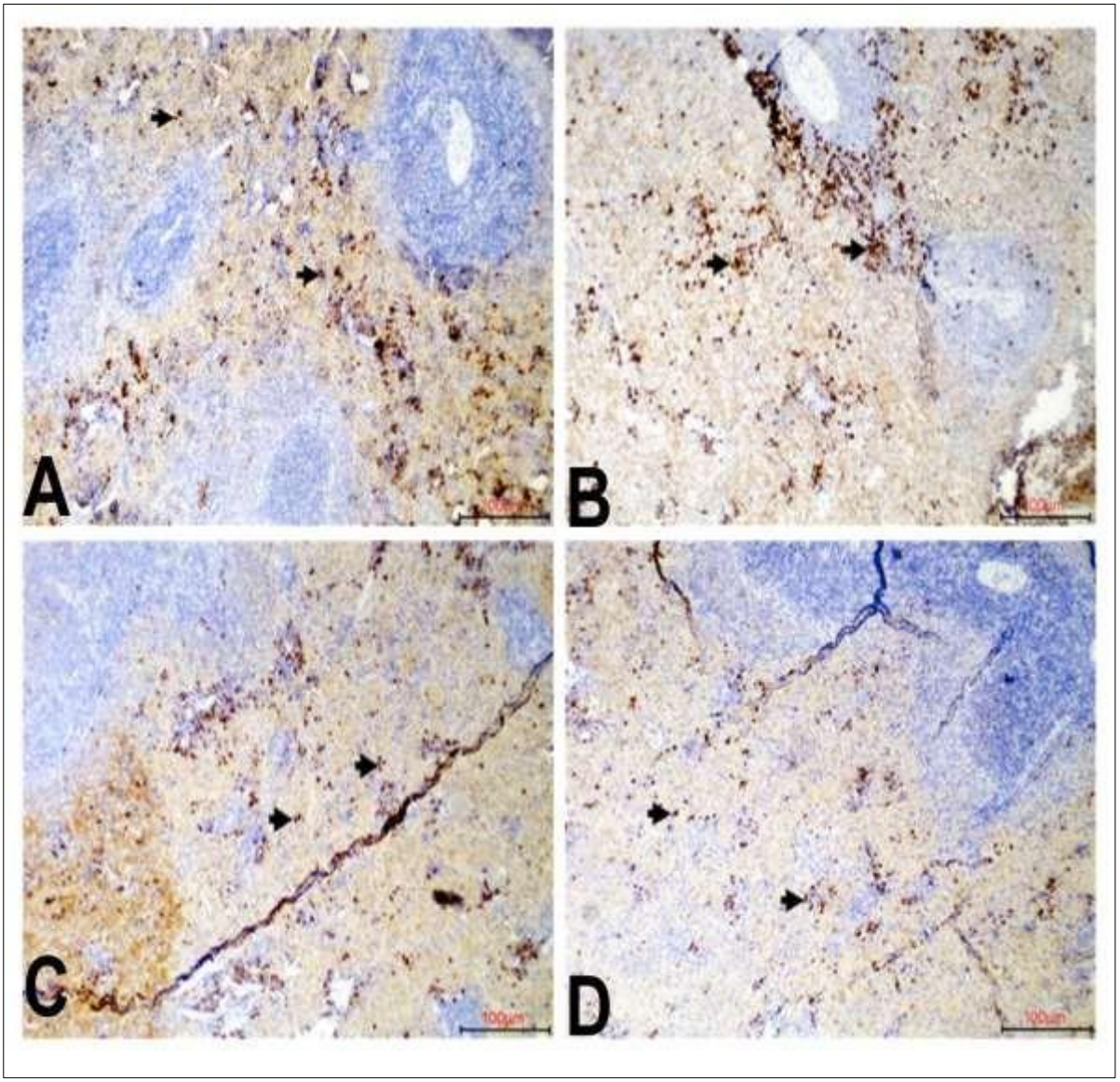

Figure 9. Immunohistochemical staining for CD163 in spleens of control and experimental rats**.** (A) Control rats showing very high immunoreactivity (++++) of CD163, evident as brown staining in a normal resident subset of splenic macrophages within the red pulp (black arrows). (IHC, 100 µm). (B) Rats exposed to continuous light showing very high immunoreactivity (++++) of CD163, with increased expression compared to controls, localized in splenic macrophages of the red pulp (black arrows). (IHC, 100 µm). (C) Rats exposed to continuous light and treated with melatonin (10 mg/kg) showing very high immunoreactivity (++++) of CD163 in splenic macrophages (black arrows), though expression decreased after treatment compared with the continuous light group. (IHC, 100 µm). (D) Rats exposed to continuous light and treated with ramelteon (10 mg/kg) showing very high immunoreactivity (++++) of CD163 in splenic macrophages (black arrows), with expression significantly reduced after treatment compared with the continuous light group. (IHC, 100 µm).

Table 1. Imunohistochemical scoring of CD163.

Criteria	0+	1+	2+	3+	4+
CD163	Negative - 0 cells/field	Weak ± 1 to 5 cells/field	Positive + 6 to 10 cells/field	Positive ++ 11 to 25 cells/field	Positive +++ More 25 cells/field

Note; (-) no immunoreactivity; (±) very weak immunoreactivity; (+) low positive immunoreactivity; (++) moderate immunoreactivity; (+++) high immunoreactivity; (++++) very high immunoreactivity.

Table 2. CD163 scoring in three fields/ slide

	Control	Continuous light	Continuous light & melatonin	Continous light & Ramelteon
Spleen	49, 36, 40	84, 72, 95	43, 47, 55	27, 35, 33
Adrenal gland	0, 0, 0	6, 5, 9	0, 0, 0	0, 0, 0
Thyroid gland	1, 0, 0	17, 22, 12	6, 8, 4	4, 2, 5

Effect of melatonin on thyroid gland of pinealectomized rats

In the control rats, histological sections of the thyroid gland displayed normal follicles of variable sizes, each lined by a single layer of cuboidal follicular cells (black arrows) containing acidophilic colloid (blue arrows). Interfollicular regions contained connective tissue with small blood vessels, while parafollicular cell groups were also evident between follicles (red arrows), confirming normal thyroid organization (Figure 10A–B). In contrast, pinealectomized rats exhibited structural disorganization of the thyroid follicles. Some follicles appeared irregular and enlarged (black arrows), with extensive connective tissue deposition between them (blue arrows). Blood vessels were congested and dilated, reflecting vascular disturbances (red arrows) (Figure 10C). In other sections, follicles were lined by flattened epithelial cells with nuclei displaced along the basement membrane (black arrows), while interfollicular connective tissue appeared increased (blue arrows), indicating atrophic and degenerative changes (Figure 10D).

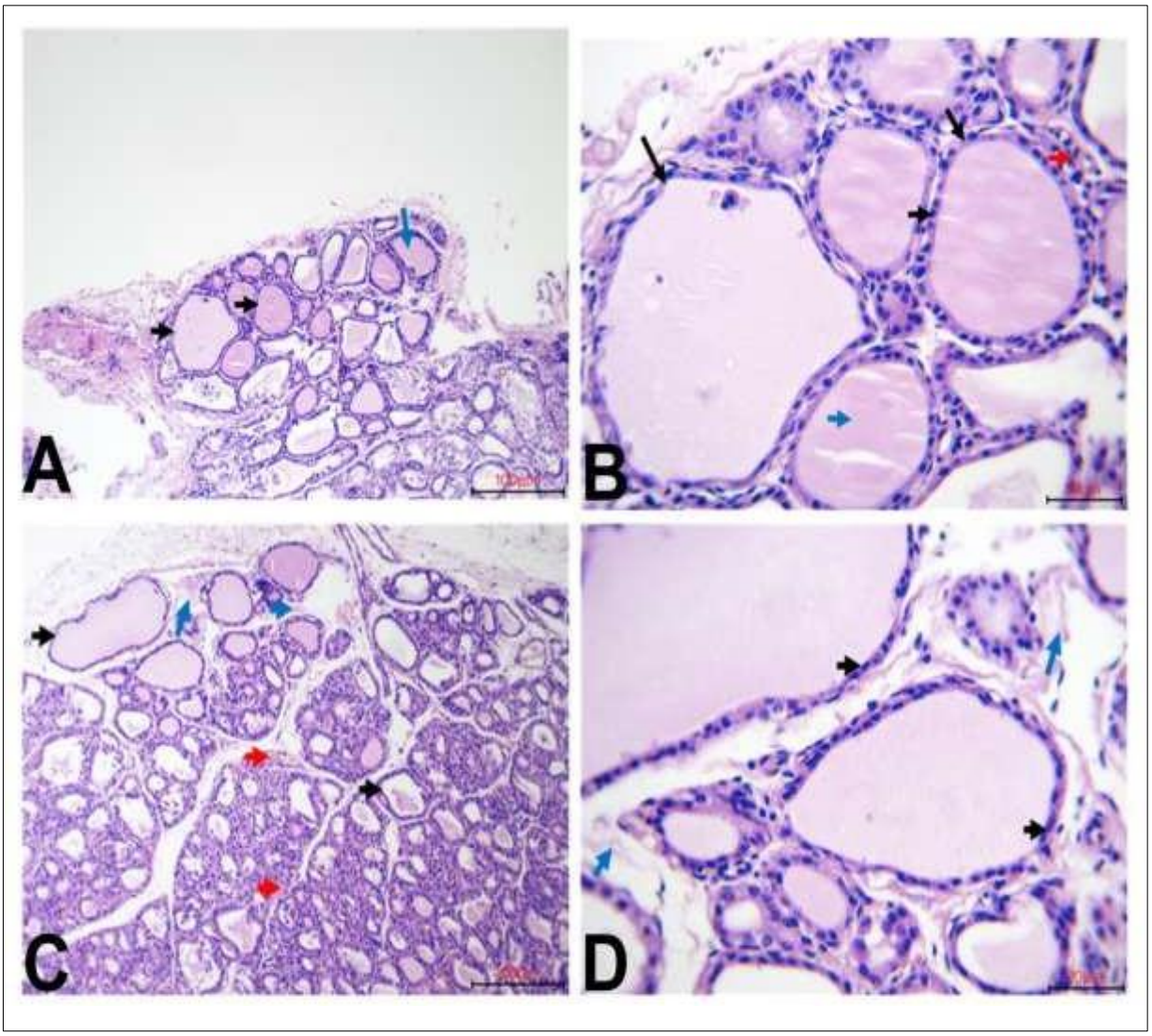

Figure 10. Histological sections of the thyroid gland in control and pinealectomized rats**.** (A) Control rats showing follicles of variable size lined by a single layer of cuboidal follicular cells (black arrows) containing acidophilic colloid (blue arrows). (H&E, 100 µm). (B) Control rats showing follicles of different sizes lined by cuboidal cells with centrally located rounded nuclei (black arrows). Follicles contain eosinophilic colloid (blue arrows), and

small groups of parafollicular cells are visible between follicles (red arrows). (H&E, 20 µm). (C) Pinealectomized rats showing irregular thyroid follicles with apparent enlargement of some follicles (black arrows), extensive connective tissue between follicles (blue arrows), and congested, dilated blood vessels (red arrows). (H&E, 100 µm). (D) Pinealectomized rats showing follicles lined with cells bearing flat nuclei (black arrows) and extensive connective tissue between follicles (blue arrows). (H&E, 20 µm).

In pinealectomized rats treated with melatonin, the thyroid gland displayed follicles of variable sizes (black arrows), most of which were lined by a single layer of cuboidal follicular epithelium (blue arrows). However, some follicles were associated with congested blood vessels in the interfollicular connective tissue (red arrows), suggesting partial restoration of vascular and epithelial organization (Figure 11A–B). In pinealectomized rats treated with ramelteon, thyroid sections showed better preservation of follicular architecture. Follicles of variable sizes were lined by cuboidal epithelial cells (blue arrows), though some areas displayed congested blood vessels (red arrows) and mild infiltration of inflammatory cells in the interfollicular regions (green arrow), indicating incomplete recovery (Figure 11C). Other sections revealed follicles lined by cuboidal cells, but with a subset of follicular cells displaced abnormally into the lumen (red arrows), reflecting localized structural alterations despite overall preservation (Figure 11D).

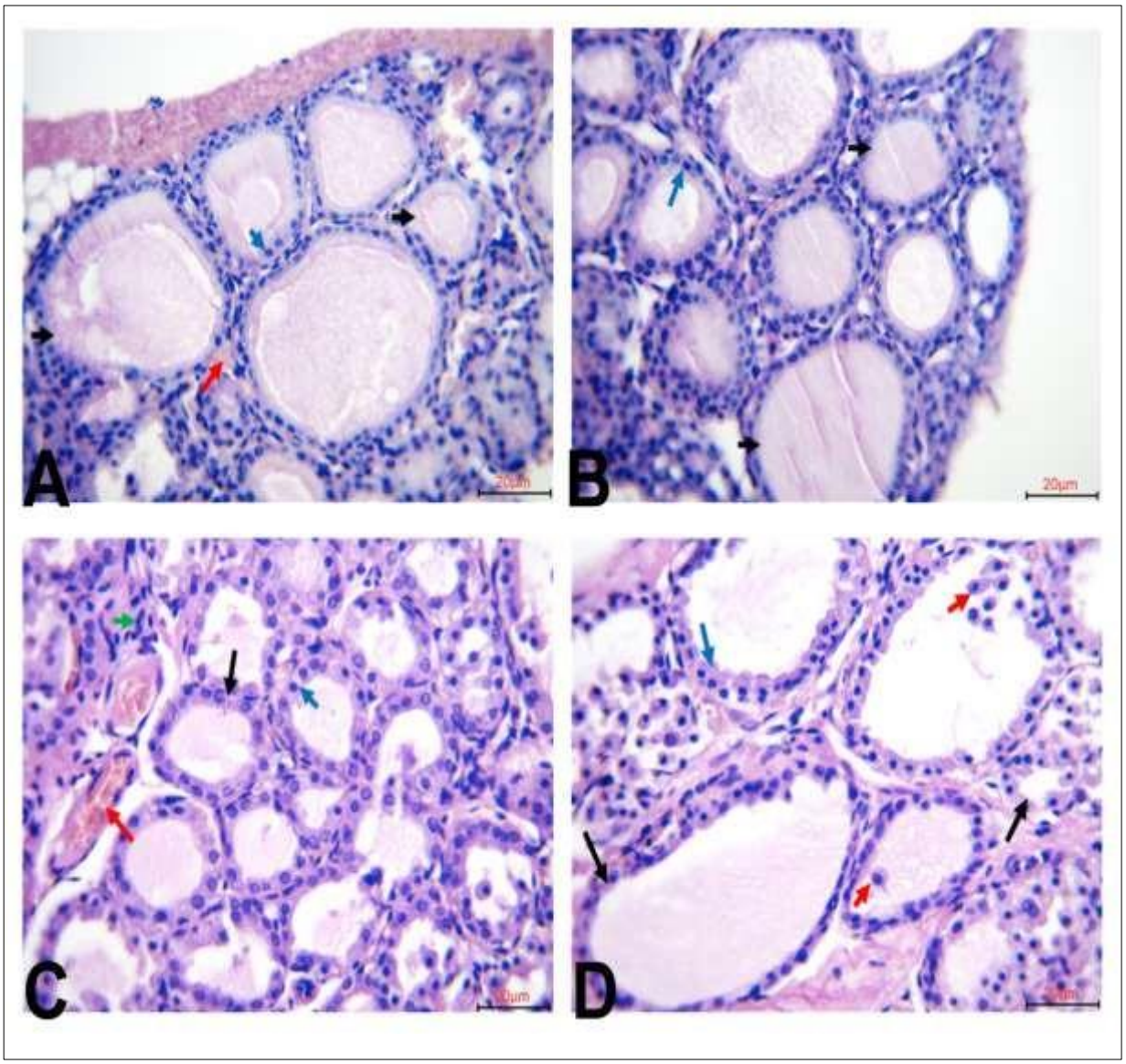

Figure 11. Histological sections of the thyroid gland in rats exposed to continuous light or pinealectomy and treated with melatonin or ramelteon**.** (A) Rats exposed to continuous light and treated with melatonin (10 mg/kg) showing follicles of variable size (black arrows) lined by a single cuboidal epithelial layer (blue arrow) and congested blood vessels (red arrow). (H&E, 20 µm). (B) Rats exposed to continuous light and treated with melatonin showing follicles of variable size (black arrows) lined by a single cuboidal follicular epithelium (blue arrow). (H&E, 20 µm). (C) Pinealectomized rats treated with ramelteon (10 mg/kg) showing normal thyroid follicles (black arrow) lined by cuboidal follicular epithelium (blue arrow), congested blood vessels (red arrow),

and infiltration of inflammatory cells (green arrow). (H&E, 20 µm). (D) Pinealectomized rats treated with ramelteon showing follicles of variable size (black arrows) lined by cuboidal follicular epithelium (blue arrow), with some follicular cells abnormally located and projecting into the follicular lumen (red arrows). (H&E, 20 µm).

In pinealectomized rats exposed to continuous light, thyroid histology revealed advanced degenerative changes. Follicles were lined by epithelial cells with flattened nuclei (black arrows), and some follicular cells exhibited vacuolated cytoplasmic degeneration. The number of parafollicular cells appeared increased (blue arrow), indicating a reactive cellular response. Markedly dilated and congested blood capillaries were observed in the interfollicular connective tissue (red arrows), reflecting vascular stress. Additionally, focal infiltration of inflammatory cells was detected around blood vessels (green arrows), suggesting an inflammatory reaction superimposed on structural damage (Figure 12).

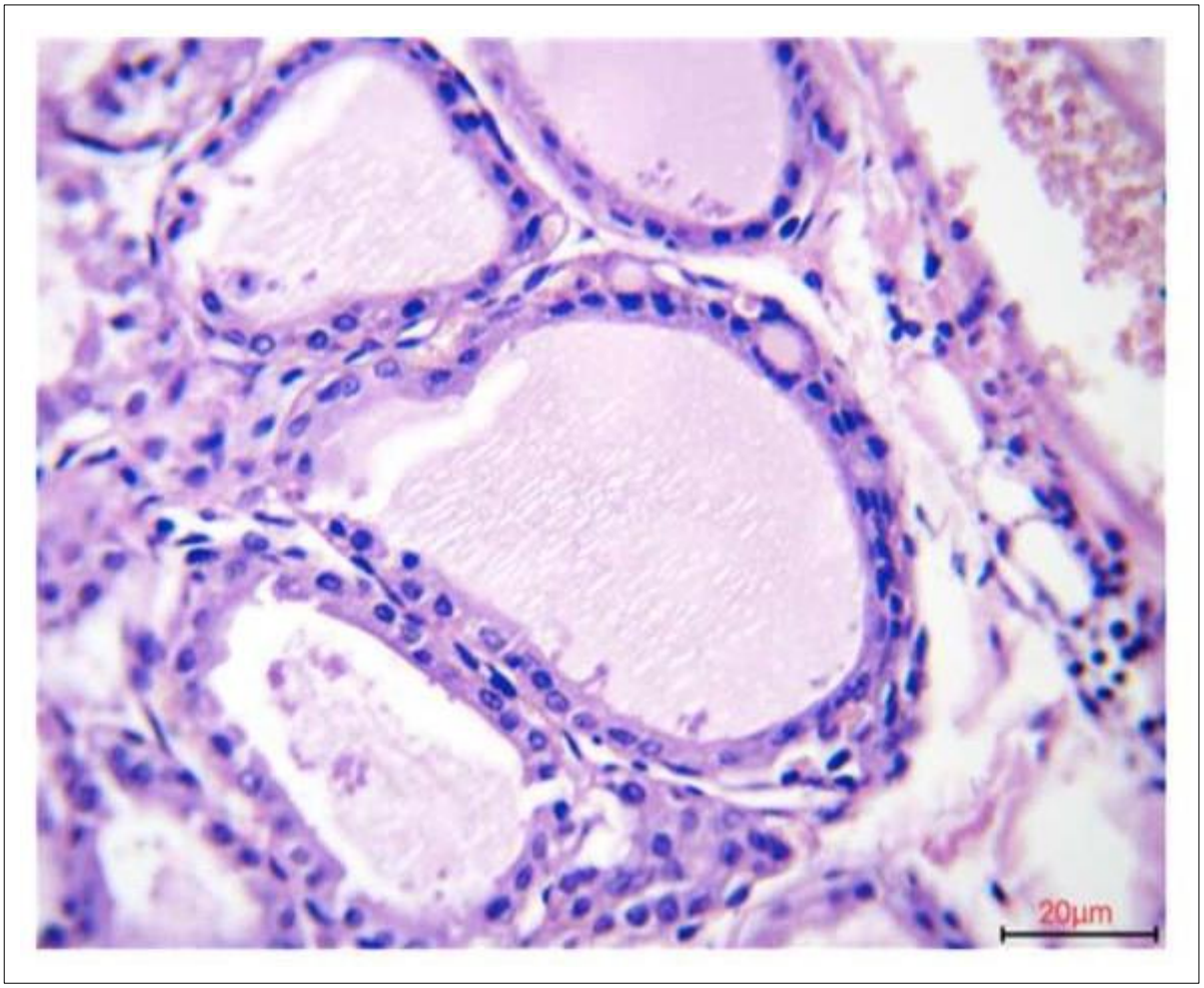

Figure 12. Histological section of the thyroid gland in pinealectomized rats exposed to continuous light. Follicles are lined with flat nuclei, with vacuolated degeneration in some follicular cells (black arrows). An increased number of parafollicular cells are visible (blue arrow), along with markedly dilated and congested blood capillaries (red arrow). Infiltration of focal inflammatory cells is observed around the blood vessels (green arrows). (H&E, 20 µm).

Effect of melatonin on adrenal gland of pinealectomized rats

In the control rats, histological sections of the adrenal gland revealed normal cortical and medullary organization. The capsule consisted of dense irregular connective tissue containing smooth muscle (black arrow), while the zona glomerulosa (blue arrow), zona fasciculata (red arrows), and zona reticularis (green arrow) were clearly distinguished. Chromaffin cells appeared normal with intact cytoplasm and nuclei (yellow arrow), confirming preserved adrenal architecture (Figure 13A). In pinealectomized rats, however, the adrenal gland showed atrophy of all adrenocortical zones. The zona fasciculata contained hypertrophic cells with pale-staining cytoplasm (black arrows), many of which exhibited fine cytoplasmic vacuolation. These degenerative alterations reflected cortical insufficiency and structural disorganization compared with the control group (Figure 13B).

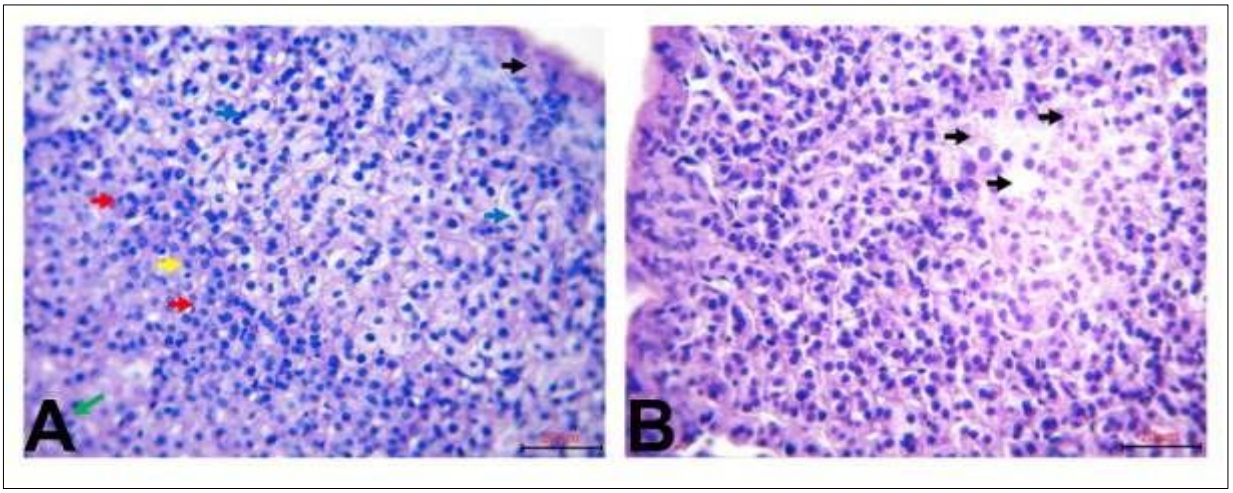

Figure 13. Histological sections of the adrenal gland in control and pinealectomized rats. (A) Control rats showing normal adrenal gland architecture with capsule of dense irregular connective tissue containing smooth muscle (black arrow), zona glomerulosa (blue arrow), zona fasciculata (red arrows), zona reticularis (green arrow), and normal chromaffin cells (yellow arrow). (H&E, 20 μm). (B) Pinealectomized rats showing atrophy of all adrenocortical zones, with focal pale-staining hypertrophic cells in the zona fasciculata (black arrows). These hypertrophic cells display finely vacuolated cytoplasm. (H&E, 20 μm).

In pinealectomized rats treated with melatonin, adrenal sections revealed near-normal cortical organization with a thin connective tissue capsule (black arrows). Only a few vacuolated cells were detected across the cortical zones (red arrows), indicating partial protection (Figure 14A). Other melatonin-treated sections showed intact cortical architecture with a thin capsule (black arrow), normal cellular arrangement without vacuolation (blue arrows), and preserved lipid droplets in the zona fasciculata (red arrows), suggesting effective restoration of cortical structure (Figure 14B). In pinealectomized rats treated with ramelteon, the adrenal gland displayed even stronger preservation. Sections showed a thin connective tissue capsule (black arrow), well-defined zona glomerulosa (blue arrows), normal zona fasciculata (red arrows), and chromaffin cells with intact lipid droplets (green arrows) (Figure 14C). Additional sections confirmed this protective effect, with normal cortical organization, a clear zona glomerulosa (blue arrow), and lipid droplets within the zona fasciculata (green arrows), reflecting a highdegree of structural recovery (Figure 14D).

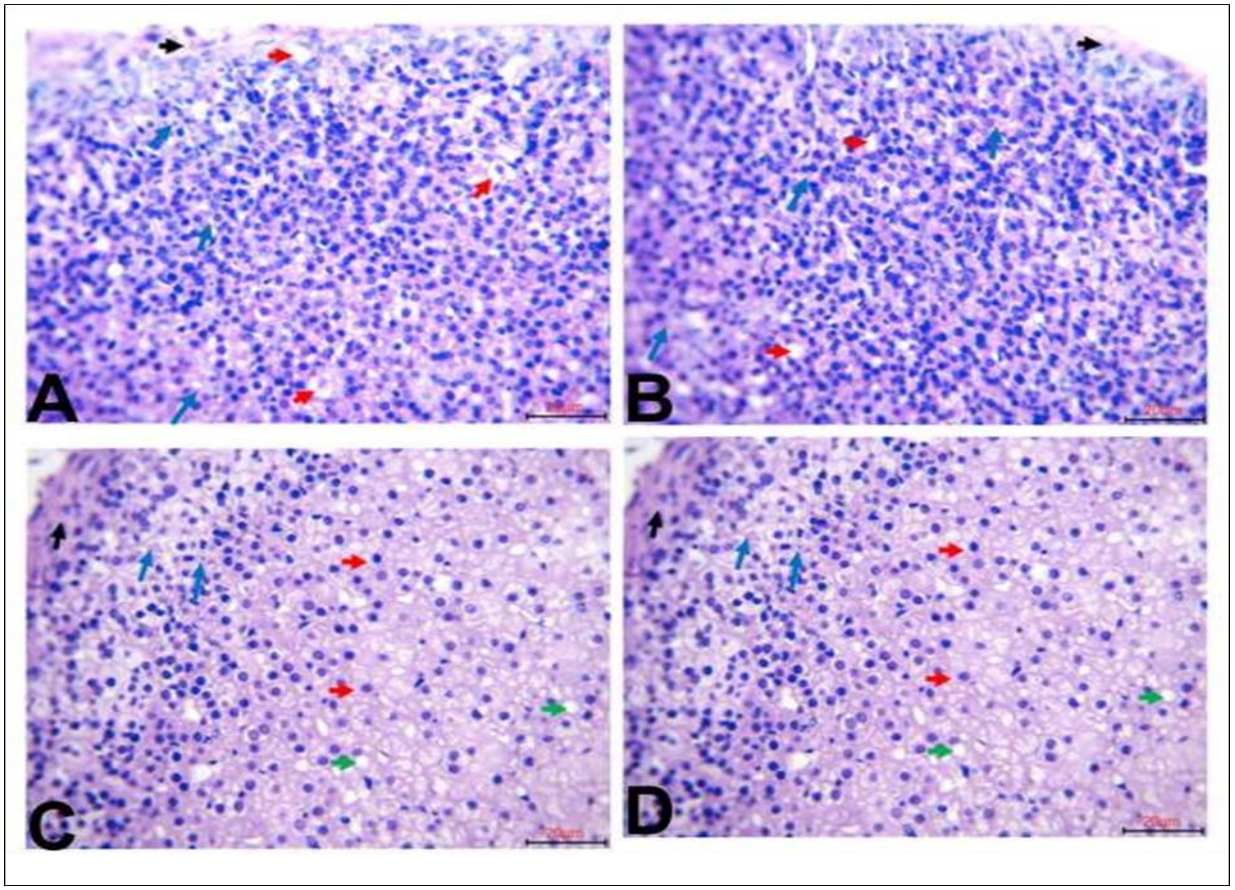

Figure 14. Histological sections of the adrenal gland in rats exposed to continuous light or pinealectomy and treated with melatonin or ramelteon. (A) Rats exposed to continuous light and treated with melatonin (10 mg/kg) showing normal adrenal cortical architecture with a thin connective tissue capsule (black arrow). Few vacuolated cells are observed within all cortical zones (red arrow). (H&E, 20 µm). (B) Rats exposed to continuous light and treated with melatonin showing normal adrenal cortical architecture with a thin connective tissue capsule (black arrow), intact cellular arrangement without vacuolation (blue arrows), and normal lipid droplets (red arrow). (H&E, 20 µm). (C) Pinealectomized rats treated with ramelteon (10 mg/kg) showing preserved adrenal gland structure with a thin connective tissue capsule (black arrow), normal zona glomerulosa (blue arrows), zona fasciculata (red arrows), and lipid droplets (green arrows). (H&E, 20 µm).
(D) Pinealectomized rats treated with ramelteon showing normal adrenal gland structure with thin connective tissue capsule (black arrow), well-defined zona glomerulosa (blue arrow), zona fasciculata (red arrow), and normal lipid droplets (green arrows). (H&E, 20 µm).

In pinealectomized rats exposed to continuous light, adrenal histology showed pronounced degenerative alterations. The cortical cells appeared disorganized, with disrupted alignment and irregular cellular morphology. In addition, sinusoidal dilatation was clearly observed, with blood-filled sinuses distributed throughout the cortex (black arrows), indicating vascular congestion and impaired tissue homeostasis (Figure 15).

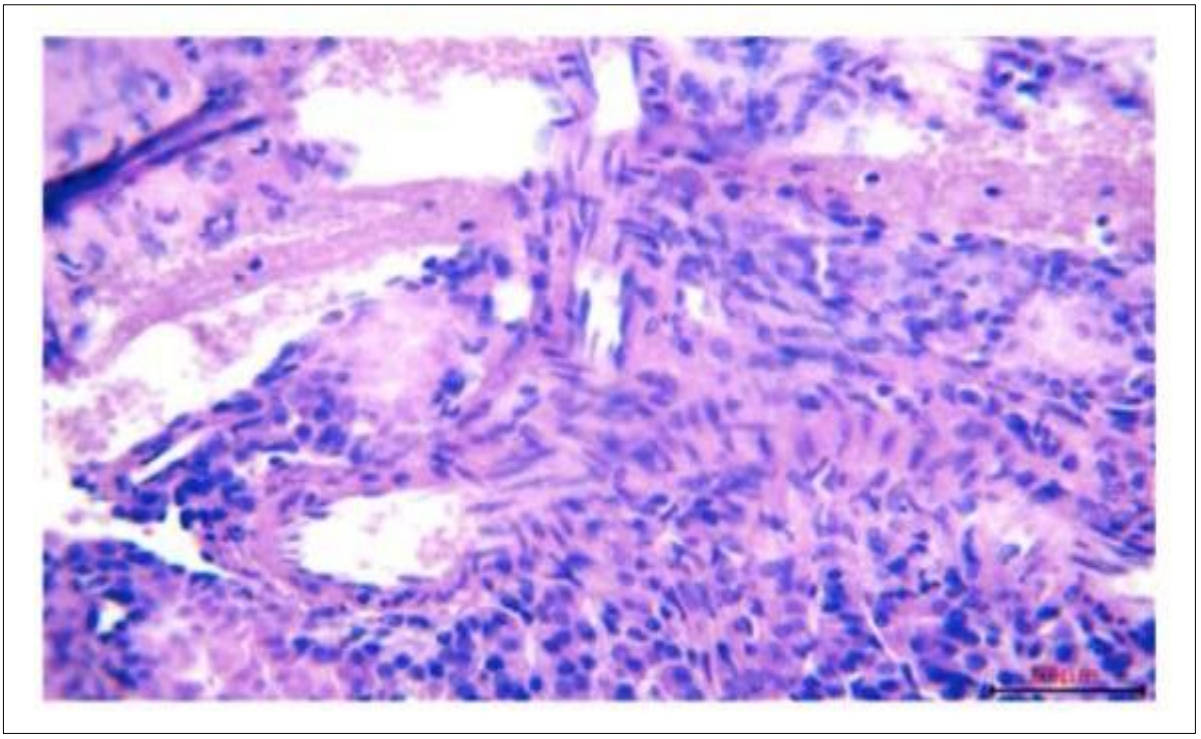

Figure 15. Histological section of the adrenal gland in pinealectomized rats exposed to continuous light. The section shows disorganization of cortical cells and dilatation of sinuses containing blood (black arrows). (H&E, 20 µm).

Effect of melatonin on spleen of pinealectomized rats

In the control rats, spleen sections showed normal histological organization with clearly defined red pulp (black arrows), white pulp or splenic nodules (blue arrows), central arteries (red arrows), and germinal centers (green arrows). The splenic architecture appeared intact, with no evidence of degeneration or congestion (Figure 16A–B). In pinealectomized rats, however, the spleen revealed significant pathological alterations. Sections showed focal areas of coagulative necrosis characterized by eosinophilic and pale-staining cells (black arrows). There was intense red blood cell congestion and hemorrhage (blue arrows), along with focal deposition of fibrinous eosinophilic material (red arrows), indicating severe vascular and parenchymal injury (Figure 16C). Additional sections confirmed these findings, with widespread coagulative necrosis, heavy congestion, and hemorrhage, as well as infiltration of inflammatory cells within the splenic tissue (green arrows) (Figure 16D).

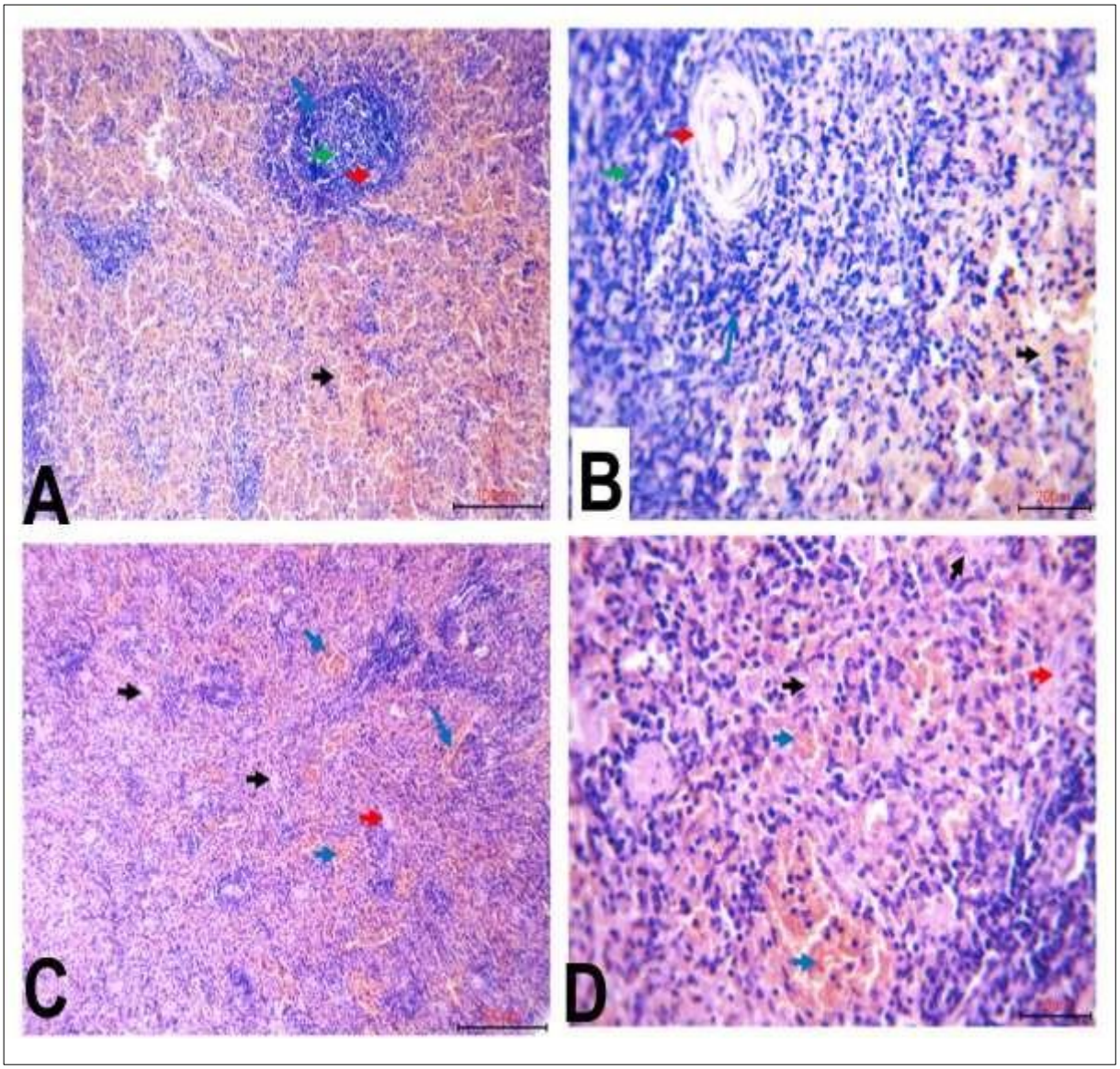

Figure 16. Histological sections of the spleen in control and pinealectomized rats. (A–B) Control rats showing normal splenic architecture with red pulp (black arrows), white pulp or splenic nodules (blue arrows), central artery (red arrows), and germinal centers (green arrows). (H&E, 100 µm and 20 µm). (C) Pinealectomized rats showing focal areas of coagulative necrosis with eosinophilic and pale-staining cells (black arrows), intense red blood cell congestion and hemorrhage (blue arrows), and focal deposition of fibrinous eosinophilic material (red arrow). (H&E, 100 µm). (D) Pinealectomized rats showing focal coagulative necrosis with eosinophilic and pale-staining cells (black arrows), severe red blood cell congestion and hemorrhage (blue arrows), along with infiltration of inflammatory cells (green arrows). (H&E, 20 µm).

In pinealectomized rats treated with melatonin, the spleen displayed preserved histological organization with distinct white pulp (black arrows) and red pulp (blue arrows). However, some regions of the red pulp appeared reduced in size compared with controls, suggesting only partial restoration of splenic structure (red arrows) (Figure 17A). In other melatonin-treated sections, the spleen showed closely preserved architecture with well- defined white pulp (black arrow) and red pulp (blue arrow), although vacuolated areas were observed within the splenic tissue (red arrows), reflecting mild residual alterations (Figure 17B). In pinealectomized rats treated with ramelteon, splenic architecture was more effectively preserved. Sections revealed well-organized white pulp (black arrows) and red pulp (blue arrows), with no obvious necrosis or congestion, indicating strong restoration of normal splenic morphology (Figure 17C).

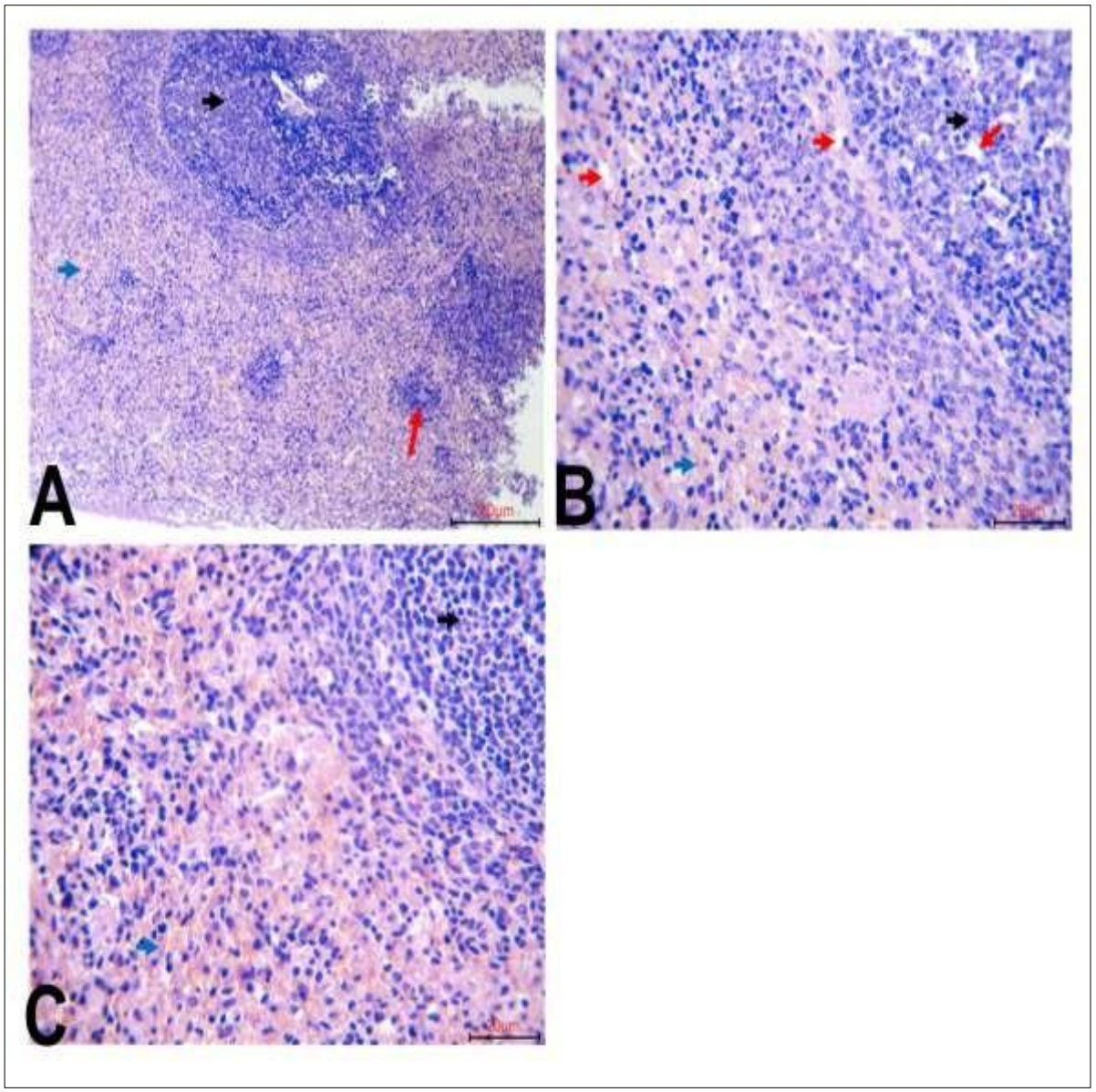

Figure 17. Histological sections of the spleen in pinealectomized rats treated with melatonin or ramelteon**.** (A) Pinealectomized rats treated with melatonin (10 mg/kg) showing preserved splenic architecture with distinct white pulp (black arrow) and red pulp (blue arrow). Some red pulp areas appear smaller compared to control (red arrow). (H&E, 100 µm). (B) Pinealectomized rats treated with melatonin showing closely preserved splenic architecture with white pulp (black arrow) and red pulp (blue arrow), but with vacuoles distributed across splenic tissue (red arrows). (H&E, 20 µm). (C) Pinealectomized rats treated with ramelteon (10 mg/kg) showing well-organized spleen with preserved architecture, including white pulp (black arrow) and red pulp (blue arrow). (H&E, 20 µm).

In pinealectomized rats exposed to continuous light, splenic histology revealed severe vascular and parenchymal damage. Sections showed marked congestion of the splenic tissue with blood-filled sinusoids and vessels (black arrows). Additionally, coagulative necrosis was evident within the red pulp (blue arrows), characterized by eosinophilic degeneration of splenic cells and loss of normal tissue architecture (Figure 18).

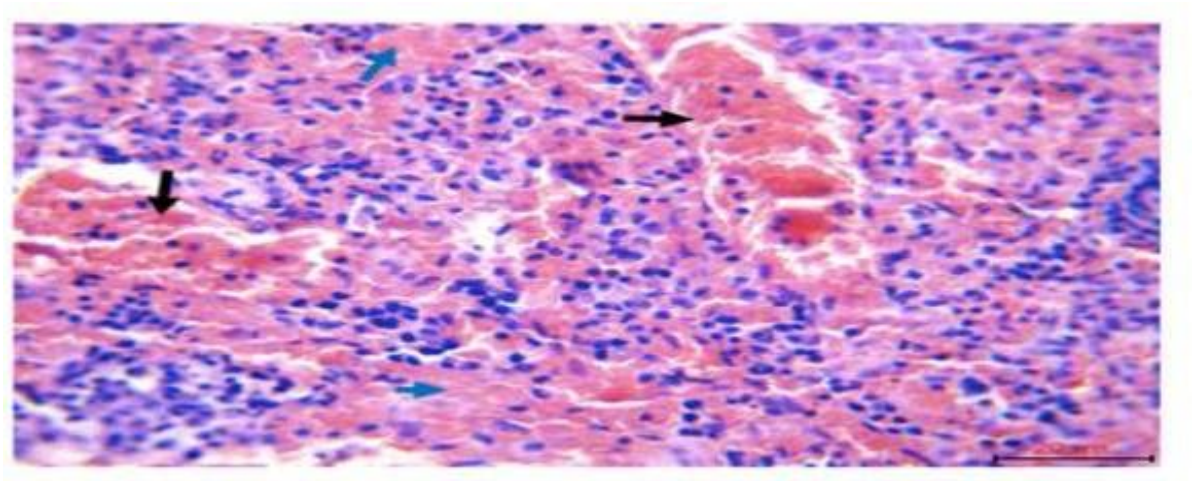

Figure 18. Histological section of the spleen in pinealectomized rats exposed to continuous light. The section shows severe congestion in the splenic tissue (black arrows) and coagulative necrosis within the red pulp (blue arrows). (H&E, 20 µm).

The CD163 immunoreactivity in thyroid gland of pinealectomized rats under different treatments

In the control rats, thyroid sections showed negative CD163 expression, with no brown staining detected in the tissue, indicating the absence of macrophage activation (Figure 19A). In pinealectomized rats, however, moderate positive CD163 immunoreactivity (++) was observed, with brown-stained infiltrating macrophages localized around thyroid follicles (black arrows), reflecting inflammatory activation (Figure 19B). Treatment with melatonin markedly reduced this response, as thyroid sections showed only very weak CD163 immunoreactivity (±), with scattered macrophages showing faint staining (black arrows), indicating partial suppression of macrophage infiltration (Figure 19C). Ramelteon treatment was even more effective, as sections revealed negative CD163 expression with no detectable brown staining, reflecting complete suppression of macrophage activity in the thyroid tissue (Figure 18D). By contrast, pinealectomized rats exposed to continuous light displayed strong positive CD163 expression (+++), characterized by numerous brown-stained infiltrating macrophages (black arrows), indicating severe macrophage-mediated inflammation (Figure 19E).

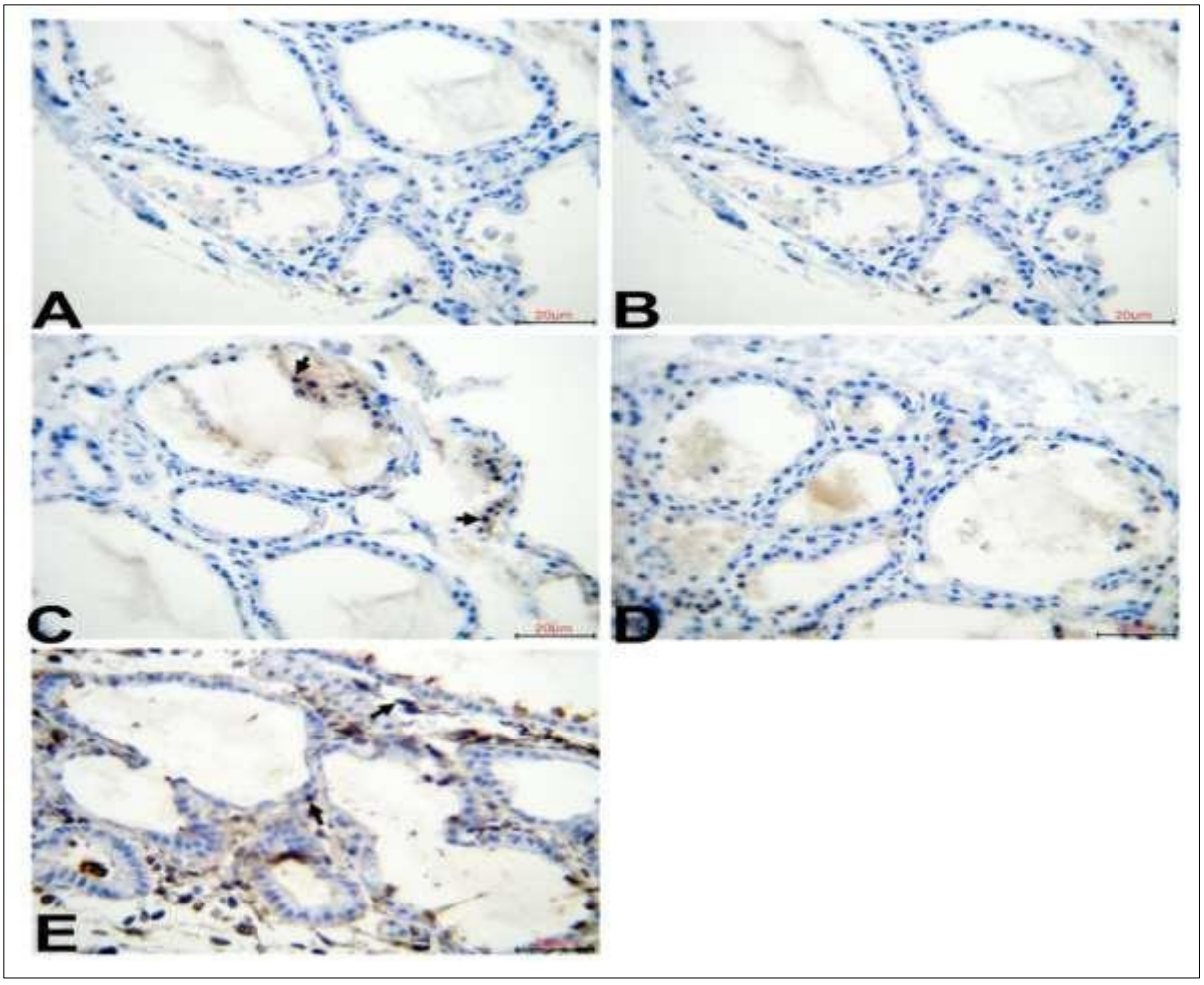

Figure 19. Immunohistochemical staining for CD163 in thyroid glands of control and pinealectomized rats under different treatments. (A) Control rats showing negative expression (–) of CD163 in thyroid tissue. (IHC, 20 µm). (B) Pinealectomized rats showing moderate positive immunoreactivity (++) of CD163, observed as brown staining in infiltrating macrophages (black arrows). (IHC, 20 µm). (C) Pinealectomized rats treated with melatonin (10 mg/kg) showing very weak immunoreactivity (±) of CD163 in infiltrating macrophages (black arrows). (IHC, 20 µm). (D) Pinealectomized rats treated with ramelteon (10 mg/kg) showing negative expression (–) of CD163 in thyroid tissue. (IHC, 20 µm). (E) Pinealectomized rats exposed to continuous light showing high immunoreactivity (+++) of CD163, evident as brown staining in infiltrating macrophages (black arrows). (IHC, 20 µm).

The CD163 immunoreactivity in adrenal gland of pinealectomized rats under different treatments

In the control rats, adrenal sections showed negative CD163 expression, with no detectable brown immunostaining, confirming the absence of macrophage activation (Figure 20A). In pinealectomized rats, low positive CD163 immunoreactivity (+) was observed, characterized by brown-stained infiltrating macrophages (black arrows) within the adrenal tissue, indicating mild inflammatory activity (Figure 20B). Following melatonin treatment, CD163 expression returned to negative levels, with no visible immunostaining in adrenal tissue, demonstrating suppression of macrophage infiltration (Figure 20C). Similarly, ramelteon treatment also produced negative CD163 expression, with adrenal sections free of brown-stained macrophages, reflecting strong immunosuppressive protection (Figure 20D). In pinealectomized rats exposed to continuous light, moderate positive CD163 immunoreactivity (++) was detected, with more pronounced brown-stained infiltrating macrophages (black arrows) compared to pinealectomy alone, indicating enhanced inflammatory activation under combined stress (Figure 20E).

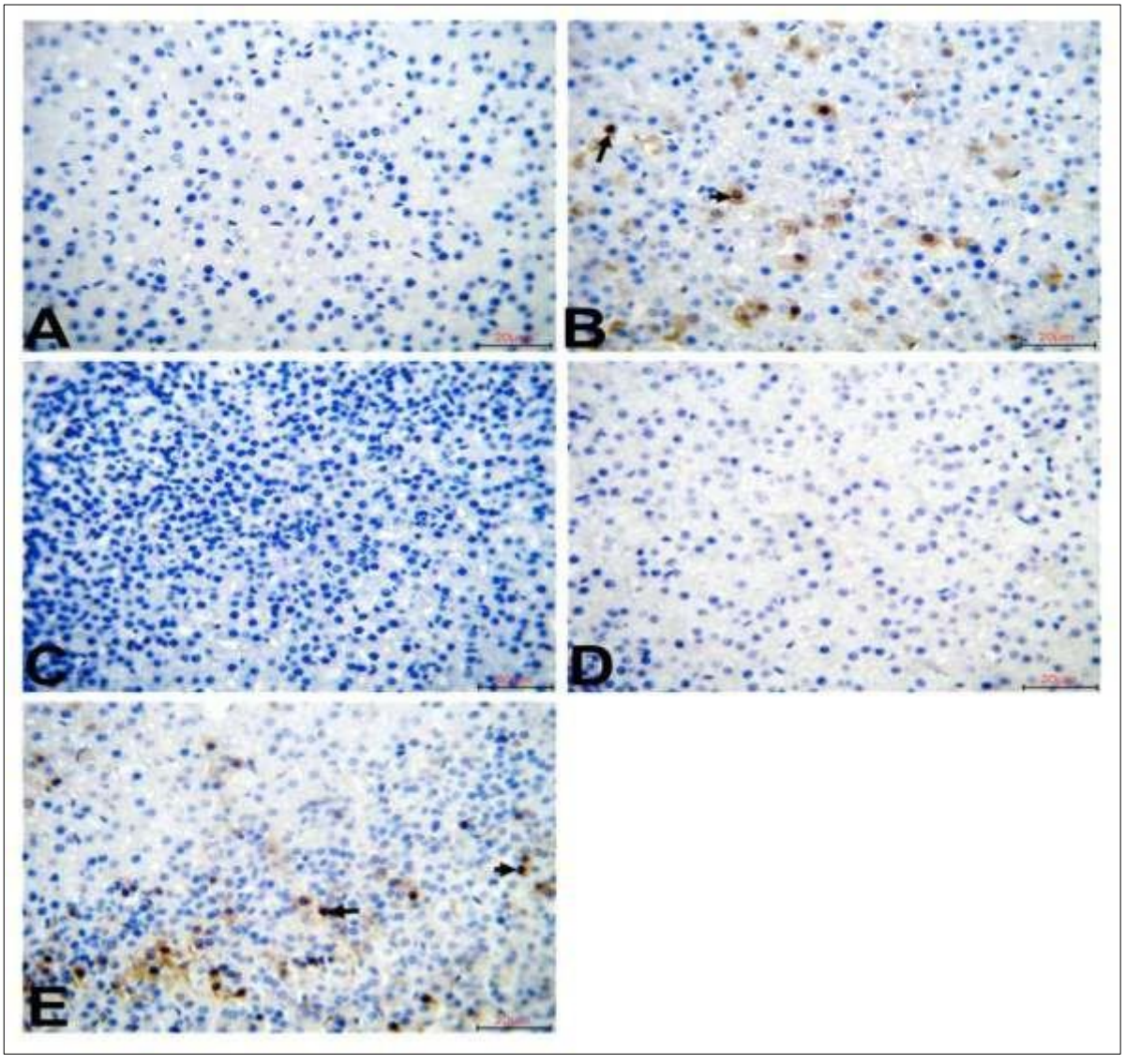

Figure 20. Immunohistochemical staining for CD163 in adrenal glands of control and pinealectomized rats under different treatments**.** (A) Control rats showing negative expression (–) of CD163 in adrenal tissue. (IHC, 20 µm). (B) Pinealectomized rats showing low positive immunoreactivity (+) of CD163, visible as brown staining in

infiltrating macrophages (black arrows). (IHC, 20 μm). (C) Pinealectomized rats treated with melatonin (10 mg/kg) showing negative expression (–) of CD163 in adrenal tissue. (IHC, 20 μm). (D) Pinealectomized rats treated with ramelteon (10 mg/kg) showing negative expression (–) of CD163 in adrenal tissue. (IHC, 20 μm). (E) Pinealectomized rats exposed to continuous light showing moderate positive immunoreactivity (++) of CD163, observed as brown staining in infiltrating macrophages (black arrows). (IHC, 20 μm).

The CD163 immunoreactivity in spleen of pinealectomized rats under different treatments

In the control rats, spleen sections exhibited moderate CD163 immunoreactivity (++), visible as brown staining in resident splenic macrophages located within both the white and red pulp (black arrows), reflecting baseline immune activity (Figure 21A). In pinealectomized rats, CD163 expression was markedly increased, with very high immunoreactivity (++++), localized in multiple subsets of splenic macrophages in both white and red pulp, indicating strong macrophage activation (Figure 21B). Following melatonin treatment, splenic sections showed reduced CD163 expression, with moderate immunoreactivity (++), evident in limited subsets of macrophages (black arrows), suggesting partial suppression of immune activation (Figure 21C). Ramelteon treatment produced an even greater reduction, with low positive immunoreactivity (+), as only scattered macrophages stained brown, reflecting stronger immunomodulation (Figure 21D). By contrast, pinealectomized rats exposed to continuous light exhibited very high CD163 immunoreactivity (++++), with extensive brown-stained macrophages distributed across both white and red pulp, confirming exacerbated immune activation (Figure 21E; Table 3, 4).

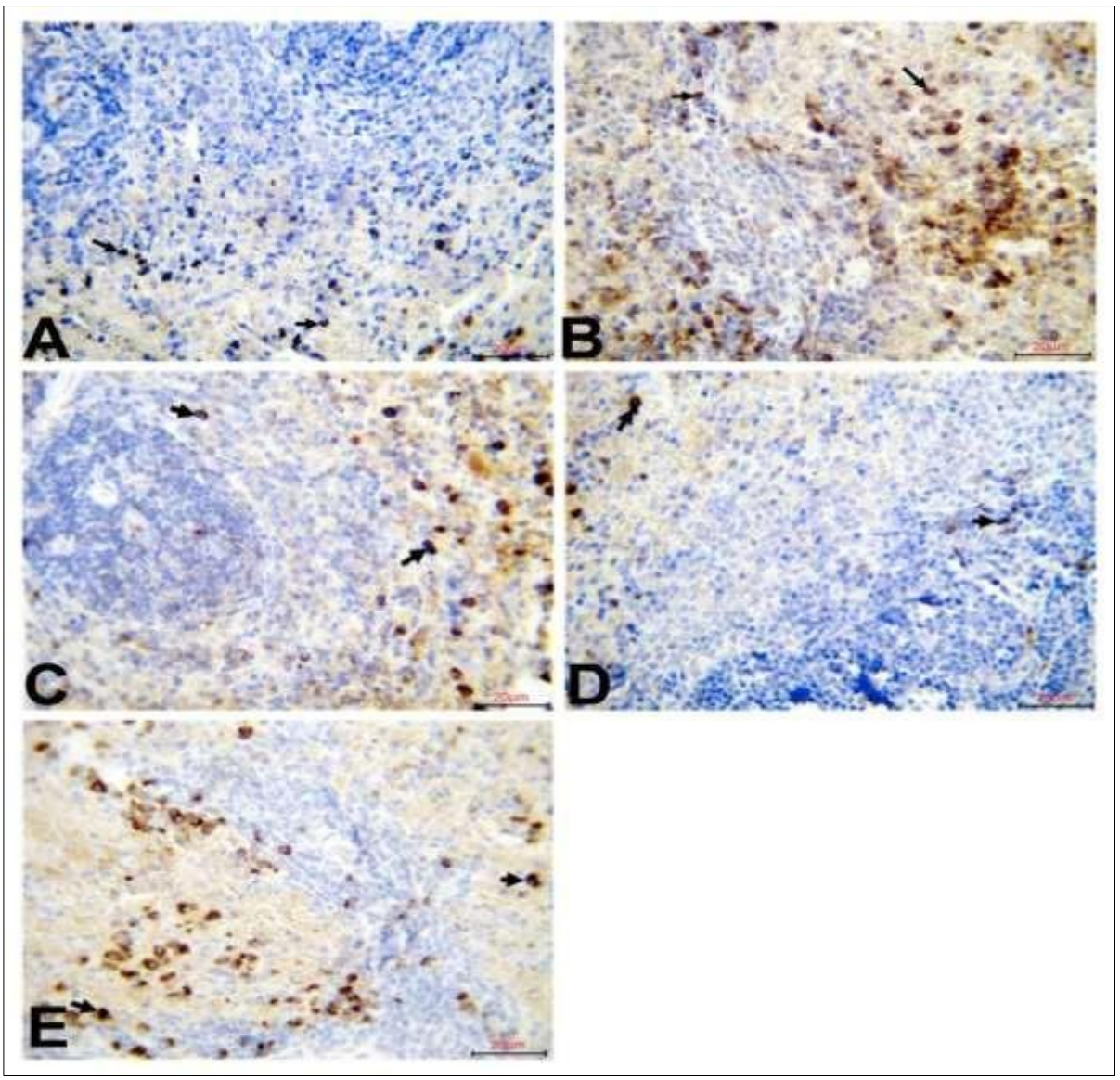

Figure 21. Immunohistochemical staining for CD163 in spleens of control and pinealectomized rats under different treatments. (A) Control rats showing moderate immunoreactivity (++) of CD163, visible as brown staining in resident splenic macrophages within both white and red pulp (black arrows). (IHC, 20 μm). (B) Pinealectomized rats showing very high immunoreactivity (++++) of CD163, localized in subsets of splenic macrophages within white and red pulp (black arrows). (IHC, 20 μm). (C) Pinealectomized rats treated with

melatonin (10 mg/kg) showing moderate immunoreactivity (++) of CD163 in subsets of splenic macrophages (black arrows). (IHC, 20 µm).
(D) Pinealectomized rats treated with ramelteon (10 mg/kg) showing low positive immunoreactivity (+) of CD163 in subsets of splenic macrophages (black arrows). (IHC, 20 µm). (E) Pinealectomized rats exposed to continuous light showing very high immunoreactivity (++++) of CD163 in subsets of splenic macrophages within both white and red pulp (black arrows). (IHC, 20 µm).

Table 3. Immunohistochemical scoring of CD163.

Criteria	0+	1+	2+	3+	4+
CD163	Negative - 0 cells/field	Weak ± 1 to 5 cells/field	Positive + 6 to 10 cells/field	Positive ++ 11 to 25 cells/field	Positive +++ More 25 cells/field

Note; (-) no immunoreactivity; (±) very weak immunoreactivity; (+) low positive immunoreactivity; (++) moderate immunoreactivity; (+++) high immunoreactivity; (++++) very high immunoreactivity.

Table 4. CD163 scoring in three fields/ slide

	Control	Pinealectomy	Pinealectomy & melatonin	Pinealectomy & ramelteon	Pinealectomy & Continuous light
Spleen	17, 20, 22	33, 42, 49	19, 16, 25	6, 8, 11	44, 32, 29
Adrenal gland	0, 0, 0	6, 5, 9	0, 0, 0	0, 0, 0	12, 14, 15
Thyroid gland	0, 0, 0	15, 24, 13	5, 4, 4	0, 0, 0	24, 22, 29

DISCUSSION

This study provides clear evidence that disruption of pineal function, whether by continuous light exposure or surgical pinealectomy, induces profound histological and immunological alterations in the thyroid, adrenal gland, and spleen of rats. Furthermore, treatment with melatonin or its receptor agonist ramelteon significantly alleviated these pathological changes, indicating their protective roles in maintaining circadian-driven endocrine and immune homeostasis. Continuous light exposure and pinealectomy caused marked changes in the thyroid, including irregular follicles, colloid depletion, epithelial cell hyperplasia, and vascular congestion. These findings align with previous studies showing that melatonin deficiency impairs thyroid gland activity by disrupting circadian rhythmicity of thyrotropin-releasing hormone (TRH) and thyroid-stimulating hormone (TSH) secretion [12]. Light-induced suppression of melatonin has been linked to oxidative stress in follicular cells, colloid depletion, and altered thyroid hormone output [13]. Pinealectomy-induced damage, including flattened follicular epithelium and increased connective tissue, confirms the dependence of thyroid homeostasis on pineal function. Melatonin treatment largely preserved follicular structure and reduced inflammatory infiltration, consistent with its reported antioxidative and anti-apoptotic effects on thyroid tissue ([14]. Similarly, ramelteon maintained thyroid architecture with minimal vacuolation, supporting the view that melatonin receptor activation is sufficient to counteract circadian disruption. Importantly, immunohistochemical staining showed that continuous light and pinealectomy enhanced CD163-positive macrophage infiltration, reflecting tissue inflammation. Melatonin and ramelteon suppressed this infiltration, in agreement with studies showing that melatonin modulates immune cell recruitment by regulating NF-κB and cytokine signaling [15]. The adrenal gland displayed severe cortical disruption under both continuous light and pinealectomy, with hyperplasia, vacuolation, karyolysis, and chromaffin cell degeneration. These alterations may be linked to dysregulated hypothalamic–pituitary–adrenal (HPA) axis signaling under melatonin deficiency. Previous research indicates that melatonin acts as a regulator of adrenal steroidogenesis, with pinealectomy leading to elevated corticosterone and structural adrenal changes [16]. Chronic light exposure may exacerbate these effects by continuously suppressing endogenous melatonin and disrupting circadian HPA rhythmicity [17]. Treatment with melatonin restored adrenal architecture and reduced vacuolation, while ramelteon achieved nearly complete preservation of zonal structure and lipid droplet distribution. This demonstrates that the protective effect is receptor-mediated, consistent with reports that melatonin receptor agonists prevent glucocorticoid imbalance and protect adrenal cortical cells from oxidative injury [18]. CD163 immunohistochemistry revealed increased macrophage infiltration in continuous light– and pinealectomy-exposed adrenals, which was reversed by melatonin and ramelteon. Since CD163 marks anti-inflammatory M2 macrophages, its upregulation may reflect a compensatory response to tissue damage [19]. Nonetheless, the reduction after treatment suggests lowered tissue stress and reduced immune activation. The spleen was highly sensitive to circadian disruption. Continuous light and pinealectomy caused severe structural damage, including coagulative necrosis, vascular congestion, hemorrhage, fibrin deposition, and sinusoidal

dilatation. These findings corroborate earlier studies showing that circadian disruption alters splenic microarchitecture, impairs white/red pulp balance, and compromises lymphoid tissue integrity [20, 21]. Both melatonin and ramelteon treatments protected splenic architecture, though occasional vacuolations were noted. The preservation of red and white pulp suggests that melatoninergic signaling plays a role in maintaining splenic circulation and immune compartmentalization. Immunohistochemical data confirmed very high CD163 immunoreactivity in splenic macrophages under continuous light and pinealectomy, reflecting strong macrophage activation. This is consistent with melatonin deficiency promoting immune dysregulation, macrophage infiltration, and chronic inflammation [22]. Treatment with melatonin reduced CD163 expression to moderate levels, while ramelteon produced greater suppression, supporting the role of melatonin receptor agonists in regulating macrophage polarization [23]. The persistence of relatively high CD163 in treated groups may represent residual immune activation necessary for splenic function. The observed histological and immunohistochemical alterations across thyroid, adrenal gland, and spleen can be attributed to melatonin deficiency caused by either continuous light exposure or pinealectomy. Melatonin is a key circadian regulator with potent antioxidant, anti-inflammatory, and cytoprotective properties [24]. Its absence enhances oxidative stress, disrupts neuroendocrine signaling, and induces immune dysregulation. CD163-positive macrophages, associated with tissue repair and immune modulation, were markedly elevated in damaged tissues, suggesting their recruitment as a response to injury. Treatment with melatonin and ramelteon attenuated this response, demonstrating reduced tissue stress and immune activation. Together, these findings highlight the critical role of the pineal gland and melatoninergic signa+ling in maintaining endocrine–immune homeostasis. Disruption of circadian rhythms by light-at-night or pinealectomy caused multi-organ histological damage and macrophage activation, while supplementation with melatonin or ramelteon mitigated these effects. These results align with prior evidence linking circadian disruption to endocrine dysfunction and immune pathology [25, 26]. Importantly, ramelteon showed efficacy comparable to melatonin, emphasizing its therapeutic potential as a melatonin receptor agonist in managing circadian rhythm–associated disorders.

CONCLUSION

The present study demonstrates that disruption of pineal function, either by continuous light exposure or pinealectomy, induces profound histological alterations and heightened macrophage activation in the thyroid, adrenal gland, and spleen of rats. These pathological changes were characterized by follicular disorganization and colloid depletion in the thyroid, cortical vacuolation and chromaffin cell damage in the adrenal gland, and necrosis, congestion, and hemorrhage in the spleen, accompanied by marked increases in CD163-positive macrophages. Treatment with melatonin or its receptor agonist ramelteon effectively mitigated these alterations, preserving tissue architecture and reducing inflammatory responses. These findings emphasize the pivotal role of melatoninergic signaling in maintaining circadian rhythm–dependent endocrine and immune homeostasis. Moreover, the comparable efficacy of ramelteon to melatonin highlights its potential clinical application as a therapeutic agent in conditions associated with circadian disruption, endocrine dysfunction, and immune imbalance. Further investigations are warranted to explore the molecular pathways underlying these protective effects and to validate the translational significance of melatonin receptor agonists in human health.

Acknowledgments

The authors would like to express their sincere gratitude to the staff of the Advanced Animal Physiology Laboratory, College of Science, Salahaddin University-Erbil**,** Iraq for their invaluable technical assistance and support during the experimental procedures. Their contributions in maintaining the animal facility, providing laboratory resources, and ensuring the successful completion of this study are deeply appreciated.

Funding:

The authors declare that no external funding was received for this study.

REFERENCES

[1] N.M.S. Mahmood, A.M. Mahmood, I.M. Maulood, The roles of melatonin and potassium channels in relaxation response to ang 1–7 in diabetic rat isolated aorta, Cytotechnology 77(2) (2025) 55.

[2] E.B. Othman, I.M. Maulood, The impact of melatonin and its agonist on endothelin-1 reactivity in isolated aorta in continuous light and pinealectomized rats, Zanco Journal of Pure and Applied Sciences 35(2) (2023) 181-188.

[3] S. Samanta, Physiological and pharmacological perspectives of melatonin, Archives of physiology and biochemistry 128(5) (2022) 1346-1367.

[4] A. Sánchez, A.C. Calpena, B. Clares, Evaluating the oxidative stress in inflammation: role of melatonin, International journal of molecular sciences 16(8) (2015) 16981-17004.

[5] M.Z. Khan, W. Chen, X. Liu, X. Kou, A. Khan, R.U. Khan, M. Zahoor, C. Wang, An Overview of Bioactive Compounds' Role in Modulating the Nrf2/Keap1/NF-κB Pathway to Alleviate Lipopolysaccharide-Induced Endometritis, International Journal of Molecular Sciences 25(19) (2024) 10319.

[6] K. Yanar, B. Simsek, U. Çakatay, Integration of melatonin related redox homeostasis, aging, and circadian rhythm, Rejuvenation Research 22(5) (2019) 409-419.

[7] J. Tchekalarova, R. Tzoneva, Oxidative stress and aging as risk factors for Alzheimer's disease and Parkinson's disease: the role of the antioxidant melatonin, International journal of molecular sciences 24(3) (2023) 3022.
[8] C.C. Capen, T.J. Rosol, Recent advances in the structure and function of the parathyroid gland in animals and the effects of xenobiotics, Toxicologic pathology 17(2) (1989) 333-345.
[9] S. Naqvi, D. Kumar, R.K. Paul, V. Sejian, Environmental stresses and livestock reproduction, in: Environmental stress and amelioration in livestock production, Springer2012, pp. 97-128.
[10] S. Sarkar, A. Chattopadhyay, D. Bandyopadhyay, Melatonin as a promising agent alleviating endocrine deregulation and concurrent cardiovascular dysfunction: a review and future prospect, Melatonin Research 7(1) (2024) 1-19.
[11] D. García-Bernal, S. López-García, J.L. Sanz, J. Guerrero-Gironés, E.M. García-Navarro, J.M. Moraleda, L. Forner, F.J. Rodríguez-Lozano, Melatonin treatment alters biological and immunomodulatory properties of human dental pulp mesenchymal stem cells via augmented transforming growth factor beta secretion, Journal of Endodontics 47(3) (2021) 424-435.
[12] K. Ikegami, S. Refetoff, E. Van Cauter, T. Yoshimura, Interconnection between circadian clocks and thyroid function, Nature Reviews Endocrinology 15(10) (2019) 590-600.
[13] J.A. Ramaraj, S. Narayan, Anti-aging strategies and topical delivery of biopolymer-based nanocarriers for skin cancer treatment, Current Aging Science 17(1) (2024) 31-48.
[14] S.M. Mousavi, L. Etemad, D. Yari, M. Hashemi, Z. Salmasi, Evaluation of Melatonin and its Nanostructures Effects on Skin Disorders Focused on Wound Healing, Mini Reviews in Medicinal Chemistry 24(20) (2024) 1856-1881.
[15] N. Ma, J. Zhang, R.J. Reiter, X. Ma, Melatonin mediates mucosal immune cells, microbial metabolism, and rhythm crosstalk: a therapeutic target to reduce intestinal inflammation, Medicinal Research Reviews 40(2) (2020) 606-632.
[16] J. Cipolla-Neto, F.G. Amaral, J.M. Soares Jr, C.C. Gallo, A. Furtado, J.E. Cavaco, I. Goncalves, C.R.A. Santos, T. Quintela, The crosstalk between melatonin and sex steroid hormones, Neuroendocrinology 112(2) (2022) 115-129.
[17] L. Tähkämö, T. Partonen, A.-K. Pesonen, Systematic review of light exposure impact on human circadian rhythm, Chronobiology international 36(2) (2019) 151-170.
[18] P. Theodosis-Nobelos, F.-N. Varra, M. Varras, E.A. Rekka, The Effects of Antioxidant Approved Drugs and Under Investigation Compounds with Potential of Improving Sleep Disorders and their Associated Comorbidities Associated with Oxidative Stress and Inflammation, Mini-Reviews in Medicinal Chemistry 25(10) (2025) 795-815.
[19] R. Hardeland, Cell polarization, migration and tissue repair: A promising field for future melatonin research, Melatonin Research 7(2) (2024) 120-133.
[20] C. Ramsey, O. Winqvist, L. Puhakka, M. Halonen, A. Moro, O. Kämpe, P. Eskelin, M. Pelto-Huikko, L. Peltonen, Aire deficient mice develop multiple features of APECED phenotype and show altered immune response, Human molecular genetics 11(4) (2002) 397-409.
[21] D. Aw, L. Hilliard, Y. Nishikawa, E.T. Cadman, R.A. Lawrence, D.B. Palmer, Disorganization of the splenic microanatomy in ageing mice, Immunology 148(1) (2016) 92-101. https://doi.org/10.1111/imm.12590.
[22] Y. Xia, S. Chen, S. Zeng, Y. Zhao, C. Zhu, B. Deng, G. Zhu, Y. Yin, W. Wang, R. Hardeland, Melatonin in macrophage biology: current understanding and future perspectives, Journal of pineal research 66(2) (2019) e12547.
[23] S. Yang, J. Wang, D. Wang, L. Guo, D. Yu, Melatonin receptor agonist ramelteon suppresses lps-induced neuroinflammation in astrocytes, ACS Chemical Neuroscience 12(9) (2021) 1498-1505.
[24] R.J. Reiter, S.A. Rosales-Corral, D.-X. Tan, D. Acuna-Castroviejo, L. Qin, S.-F. Yang, K. Xu, Melatonin, a full service anti-cancer agent: inhibition of initiation, progression and metastasis, International journal of molecular sciences 18(4) (2017) 843.
[25] K. Megha, A. Arathi, S. Shikha, R. Alka, P. Ramya, P. Mohanan, Significance of melatonin in the regulation of circadian rhythms and disease management, Molecular Neurobiology 61(8) (2024) 5541-5571.
[26] T.P. Minari, L.P. Pisani, Melatonin supplementation: new insights into health and disease, Sleep and Breathing 29(2) (2025) 169.